Synthesis and Characterization of Porous Carbon Materials and Their Application to Hydrogen Storage Materials

蓑田, 愛

https://doi.org/10.15017/1470597

出版情報：九州大学, 2014, 博士（工学）, 課程博士
バージョン：
権利関係：全文ファイル公表済

多孔性炭素材料の合成、物性評価と
水素吸蔵材料への応用

(Synthesis and Characterization of Porous Carbon Materials and Their Application to Hydrogen Storage Materials)

Department of Hydrogen Energy System

Graduate School of Engineering

Kyushu University

Ai MINODA

2014

Contents

Chapter 1

General Introduction

1.1 Hydrogen storage

From the point of view for the energy supply and the environmental problems in the world, it becomes a common view that the world requires new energy systems that can work out in harmony with the low-carbon society. In such situations, hydrogen is being considered as a promising energy carrier for the future and attracting much attention because it will contribute to energy source diversification and energy savings (Figure 1.1)[1-5].

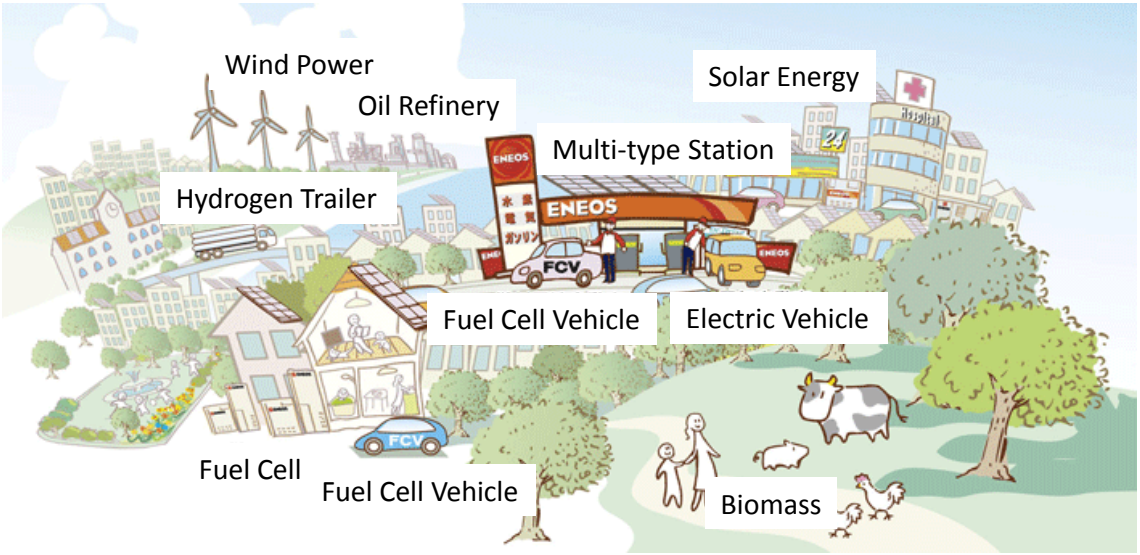

Figure 1.1. Energy in low-carbon society (reproduced with permission of JX Nippon Oil & Energy Corporation from HP)

The society where hydrogen is used as an energy carrier is called "the hydrogen society". Hydrogen is produced from various primary energies such as solar, wind and hydraulic energies as well as biomass [1]. Therefore, it will contribute to energy source diversification. Hydrogen can also be used as the media for storage and transportation of energy. Then hydrogen is fed to the fuel cells or internal combustion engines to produce energy and discard only water, emit no CO_2 during consumption (Figure 1.2). Hydrogen can generate electricity and heat efficiently when is used in a fuel cell. It can be said that hydrogen can store and re-generate electricity. For these reasons, hydrogen energy used as a fuel for fuel cells is indeed believed to be better for the energy savings and environment than the fuel combustion systems.

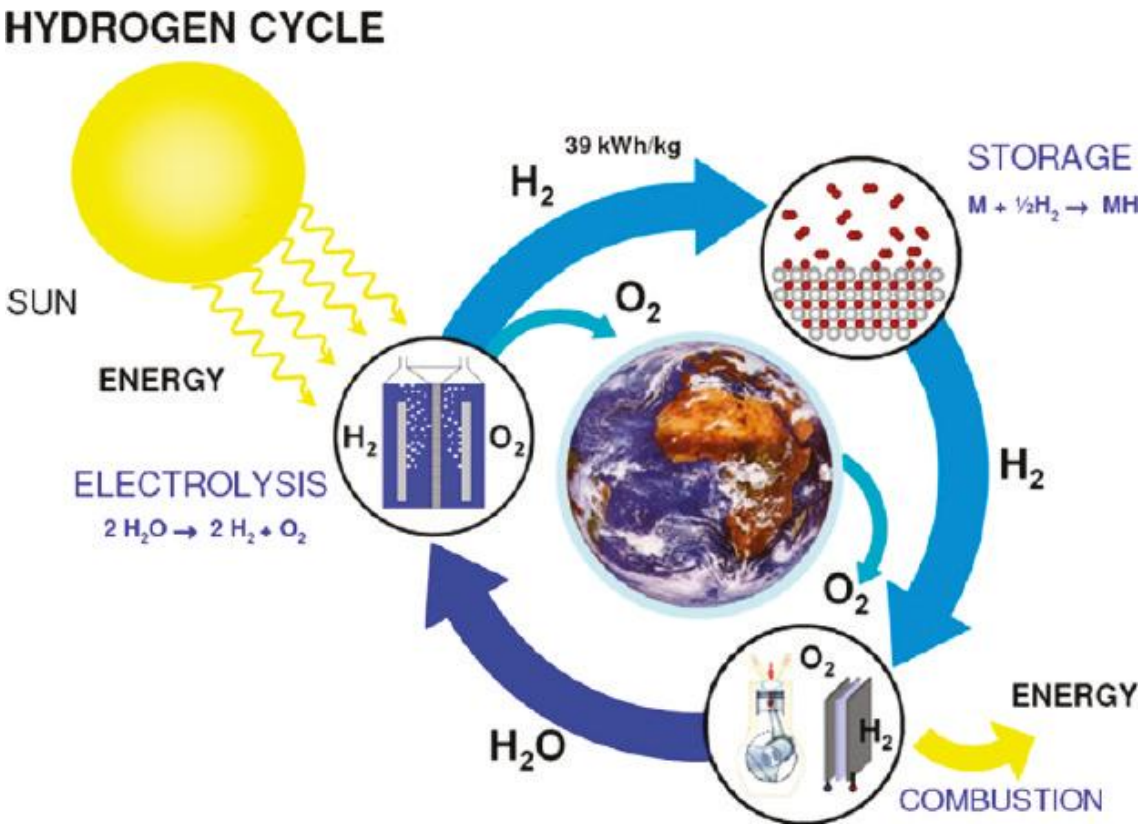

Figure 1.2. Hydrogen energy cycle [1].

However, because the volumetric energy density of hydrogen is very small, it is difficult to store and transport in a compact manner, while the gravimetric energy density is bigger than other energy carriers (Table 1.1)[2,4-5]. Generally speaking, mass quantity of ideal gas is proportional to the pressure in the same volume. However as for actual gases, even if the pressure is doubled, the quantity of molecules cannot be doubled in the same volume. The deviation from ideal gas is called compression factor. For example, when hydrogen gas is 35 MPa, the compression factor is 1.23 and when hydrogen gas is 70 MPa, the compression factor is 1.49. Thus, when each tank has the same volume and the tank pressure becomes double to 70 MPa from 35 MPa, the hydrogen mass quantity become up to only 1.6 times. Moreover, the higher the pressure is, the heavier the tank becoming and bigger the exterior content while the volume being remained, the tank should be resulting the cost turns out much expensive.

Table 1.1. Gravimetric and volumetric heat of hydrogen and other energies (higher heating values).

Energy	Volumetric energy density(MJ/m^3)	Gravimetric energy density(MJ/kg)
Hydrogen	12	142
Natural gas	39	54.5
Liquid hydrogen	10,000	142
Gasoline	34,600	49

There has been devoted much research effort to the development of ways to transport and storage hydrogen in a compact manner [2]. There are some ways to store hydrogen, such as compressed gas, liquid hydrogen, and hydrogen storage materials of hydride or hydrogen adsorption materials. Each medium have characteristics from point of the hydrogen density and hydrogen accessibility (Figure 1.3). Here, "hydrogen accessibility" means the easiness to regenerate hydrogen molecule from storage media. For example, if regeneration process needs high temperature, the accessibility is low. Liquid hydrogen has higher hydrogen density but when liquid hydrogen is produced and transported, it needs extremely low temperature (20 K) [4], much energy would be consumed during manufactures making liquid hydrogen efficiency lower than other media. Metal hydrides have higher hydrogen density but lower volumetric density because the materials are heavier than phisisorption materials. Moreover heat is also needed to regenerate hydrogen gas. The problem is the same for chemical hydrides such as ammonia. Then the hydrogen accessibility is good in the case of adsorption materials. The physisorption materials are well balanced between the points of hydrogen density and hydrogen accessibility.

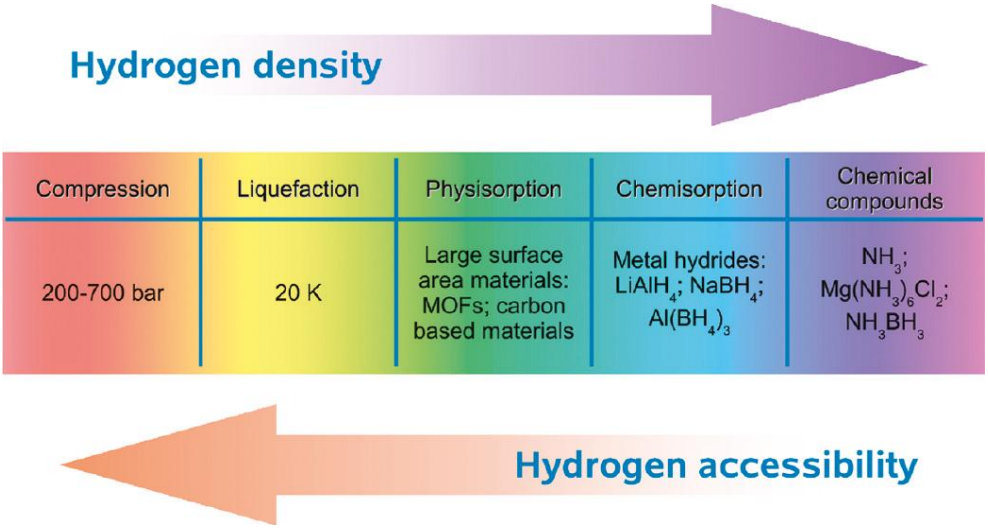

Figure 1.3. Hydrogen density and accessibility of different materials [2].

In Figure 1.4, the volumetric and gravimetric densities of various hydrogen storage media are summarized. For energy carrier, the volumetric density is important because hydrogen is generally transported within container. Liquid hydrogen has the highest hydrogen gravimetric density and the second being hydrocarbons. Hydrides have high volumetric densities that are comparable to liquid hydrogen and hydrocarbons but the gravimetric density is much lower.

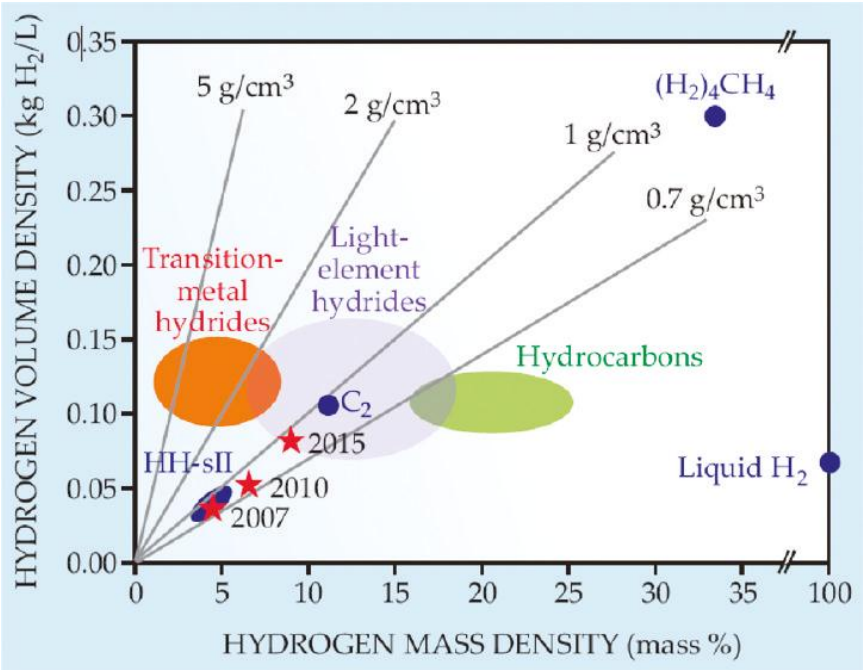

Figure 1.4. Hydrogen storage density in various chemical compounds and hydrides [3].

1.2 Physisorption materials for hydrogen storage

I focused on the physisorption materials because it have feature of balanced hydrogen density and accessibility. Physisorption materials can desorb hydrogen at an ambient temperature, so that the storage systems can be simple and heat from the outside of the system is usually not required in the desorption process. Figure 1.5 shows the features of the physisorption and chemisorption [2]. In the case of physisorption (Figure 1.5(a)), hydrogen remains molecular and binds weakly on substrate surface. Then, hydrogen can desorb easily at ambient temperatures. But in the case of the chemisorption materials (Figure 1.5(b)), hydrogen molecules dissociate to hydrogen atoms, and dissolve into materials. The chemical bonding between hydrogen and substrate is stronger than physisorption, and the enthalpy for hydrogen desorption usually became bigger.

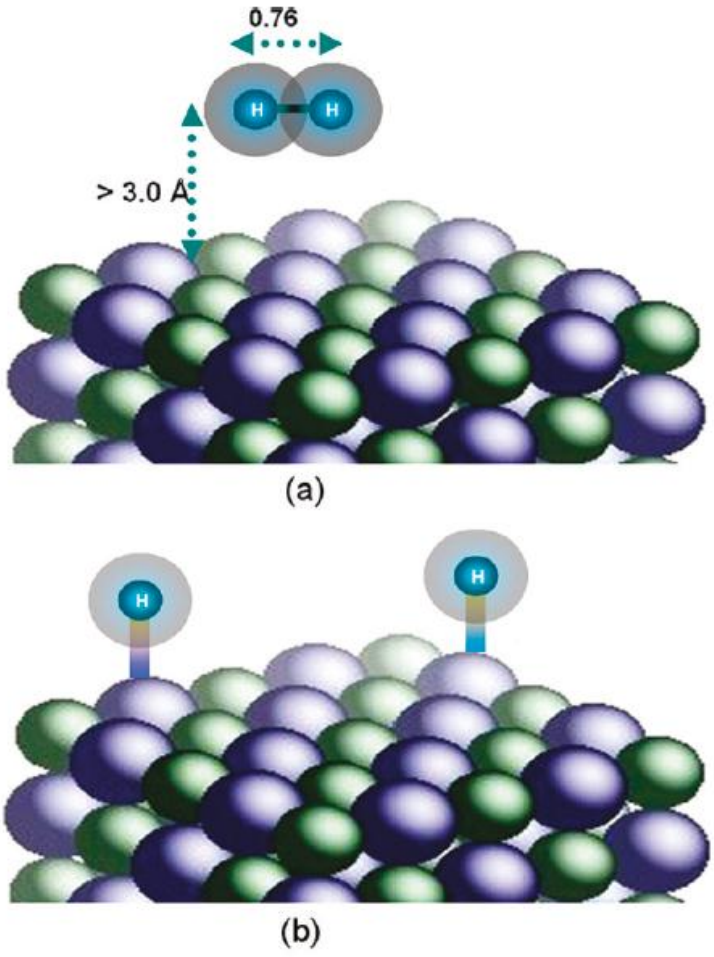

Figure 1.5. Adsorption of hydrogen on materials [2].

This feature of the physisorption materials should enable the hydrogen storage system to be energetically efficient. The comparison of heat of desorption are shown in Table 1.2. The enthalpy for hydrogen desorption is -5 kJ/mol-H_2 for physical adsorption, while -20 kJ/mol-H_2 for chemical adsorption [4]. The chemical adsorption materials need much heat for hydrogen desorption. But the amount of hydrogen adsorption is still around 1 mass% at ambient temperatures [2]. These considerations urge to develop physisorption materials of increased hydrogen storage uptake.

Table 1.2. Comparison of physical adsorption and chemical adsorption.

	Physical adsorption	Chemical adsorption
Hydrogen desorption (Enthalpy)	○ ~ -5 kJ/molH_2	× -20 ~ kJ/molH_2
Amount of hydrogen adsorption	△ 1~ mass%	○ ~7.6 mass%

1.3 Carbon materials

1.3.1 Carbon materials and their properties of hydrogen adsorotion

The development of physisorption materials for hydrogen storage has been actively pursued [6-10], most typical example being the carbon-based materials. They have strong advantages in light weight, availability and low cost, such characteristics being suitable to industrial applications.

It has been reported that materials such as carbon nanotubes [11,12], grapheme-based carbons [13-15], carbon nanofibers [16,17], and activated carbons [18-22], have shown relatively high hydrogen storage capacities under around liquid nitrogen temperature or room temperature. However at present, no one has developed carbon materials with storage capacities high enough to apply for practical applications.

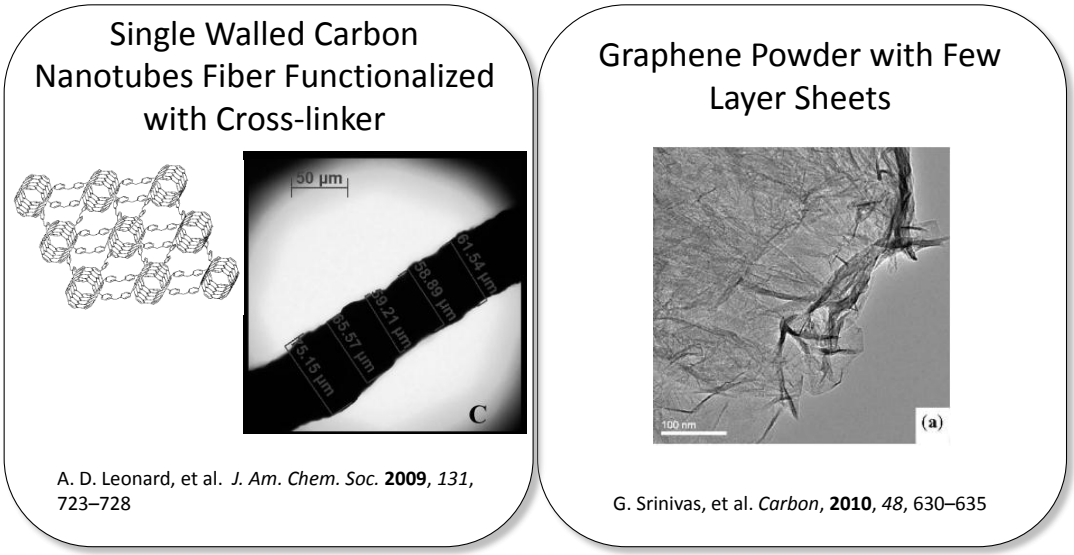

Figure 1.6. Single walled carbon nanotubes and graphene carbons [12,14].

It has been known that the relationship between the surface area and hydrogen adsorption capacity of carbon materials is almost linear at 77 K [8-10]. It has also been reported that the hydrogen adsorption capacity has a better linear relationship with the surface area at higher pressures than that at lower pressures (Figure 1.7(a)), because the available adsorption sites were almost fully saturated at 0.2 MPa. Moreover, the micropores that have under 2 nm diameters (determined by IUPAC) can provide the carbon materials a larger adsorption potential and a stronger van der Waals interaction with the hydrogen molecules. Correspondingly, the micropores may have a very important role in hydrogen storage phenomenon at higher pressures. An approximately linear relationship was actually observed between the hydrogen uptake capacity and micropore volume at 77 K and 2 MPa (Figure 1.7(b)). The result indicates that at higher pressures the pore with diameters between 1 and 2 nm may contribute more [7], which could give as good candidates for development of materials of high hydrogen storage capacities.

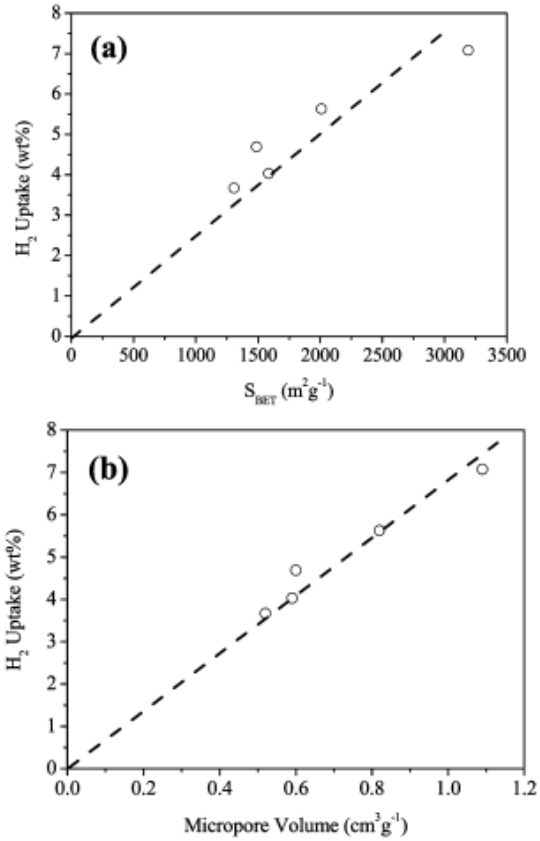

Figure 1.7. Relationships between the hydrogen uptake and BET specific surface areas (a) and micropore volumes (b) (at 77 K, 2 MPa)[7].

Relationships between hydrogen storage uptake at ambient temperature and BET specific surface areas have been also reported, linear to the BET specific surface areas. However some materials show higher hydrogen uptakes than expected from the BET results [14]. It is widely recognized that the materials with relatively high heat of adsorption show enhanced hydrogen uptakes. From these considerations, I decided the target of the research, that is, materials with medium heat of adsorption under 15 kJ/mol-H_2, not too high to chemisorption level and with adequate range of micropore distribution around 1 nm.

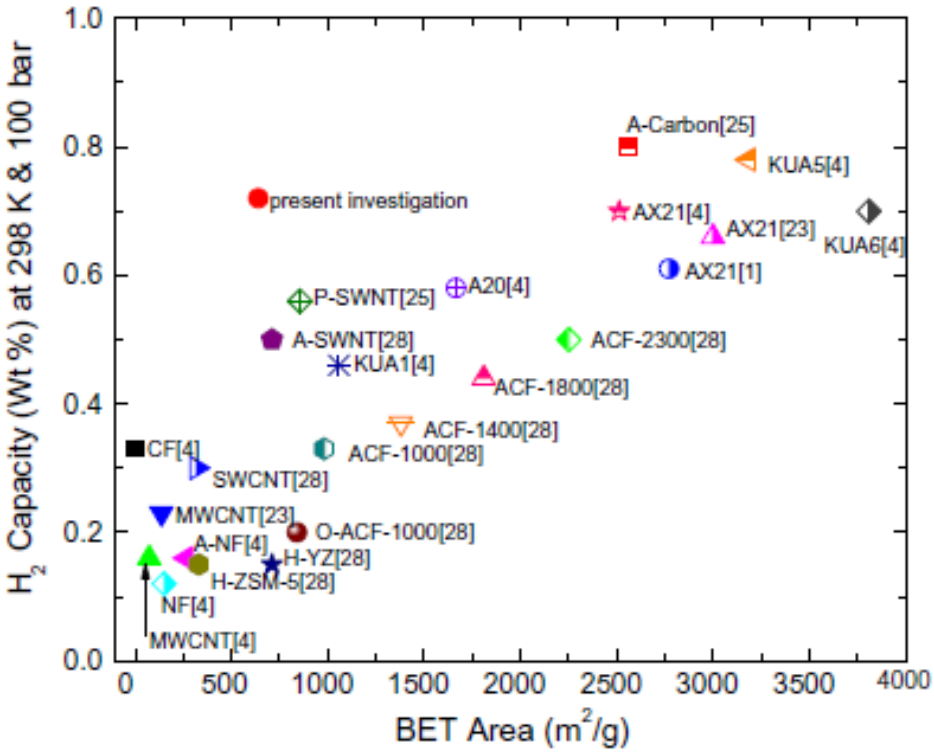

Figure 1.8. Comparison of hydrogen storage capacities with respect to the BET specific surface areas of the different carbon materials (at 298 K, 10 MPa)[14].

1.3.2 Design of carbon materials for hydrogen storage by KOH activation

As mentioned above, in order to develop the carbon materials of the micropore under 1 nm and the heat of adsorption of under 15 kJ/mol-H_2, I applied the KOH activation. KOH activation can expand the surface area [23-26], because in KOH activation process of carbon materials, the selective gasification of grapheme structures are taking place by components generated from KOH. Then, ladder-like structures formed by removal or broadening of graphene layers (Figure 1.9), followed by the rearrangement of the layers [23]. Meanwhile, pore size distribution is important for adsorption properties, needed to be controlled under around 1 nm [27]. In 303 K, KOH activated carbon that has BET surface area of 2061 m^2/g was for example, reported to adsorb relatively large amount of hydrogen, 0.62 mass% [28].

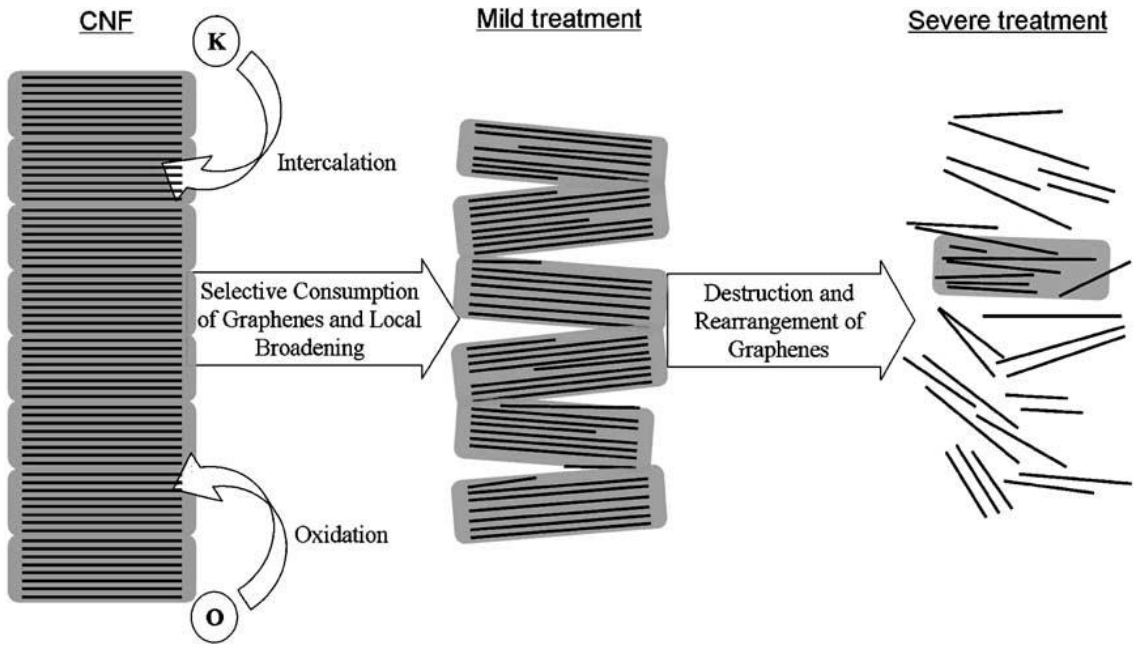

Figure 1.9. Schematic representation of KOH activation of carbon fibers [23].

Also importances are materials have the oxygen-containing functional groups on the surface of the carbon materials. These functional groups are known to have great effects on adsorption properties. So it is important to know what kind of functional groups are on the surface. The oxygen containing functional groups include mainly acidic functional groups, as shown in Figure 1.10. The oxygen containing functional groups include carboxyl, lactone, phenol, carbonyl, anhydride, ether and quinone.

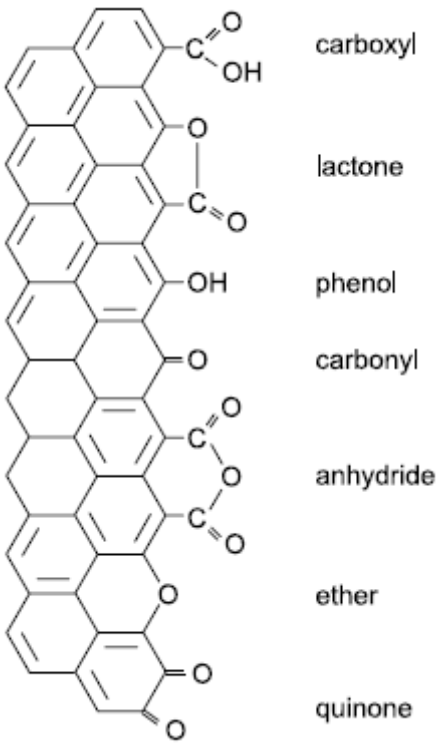

Figure 1.10. Structures of oxygen containing functional groups [33].

1.4 Lithium doping on physisorption materials

Physisorption materilals have lower heat of adsorption thane chemisorption materials, resulting in small capacities of hydrogen storage. So it was shown increasing the heat of adsorption by doping lithium atoms to some of physisorption materials. Lithium atoms have strong electron doping effect, are expected to have strong interactions with hydrogen molecules (Figure 1.11)[29-31]. Lithium doped MOFs [31], as well as carbon nanotubes [32], were examined by GCMC calculation method suggesting that the hydrogen uptake capacity will increase. When lithium was doped, heat of adsorption became around 15 kJ/mol-H_2, then, the hydrogen uptake increased at an ambient temperature such as 300 K. These studies also showed the structures of the materials have cationic charge when lithium was doped. However the cationic materials with no counter anions were thought to be hard to realize experimentally.

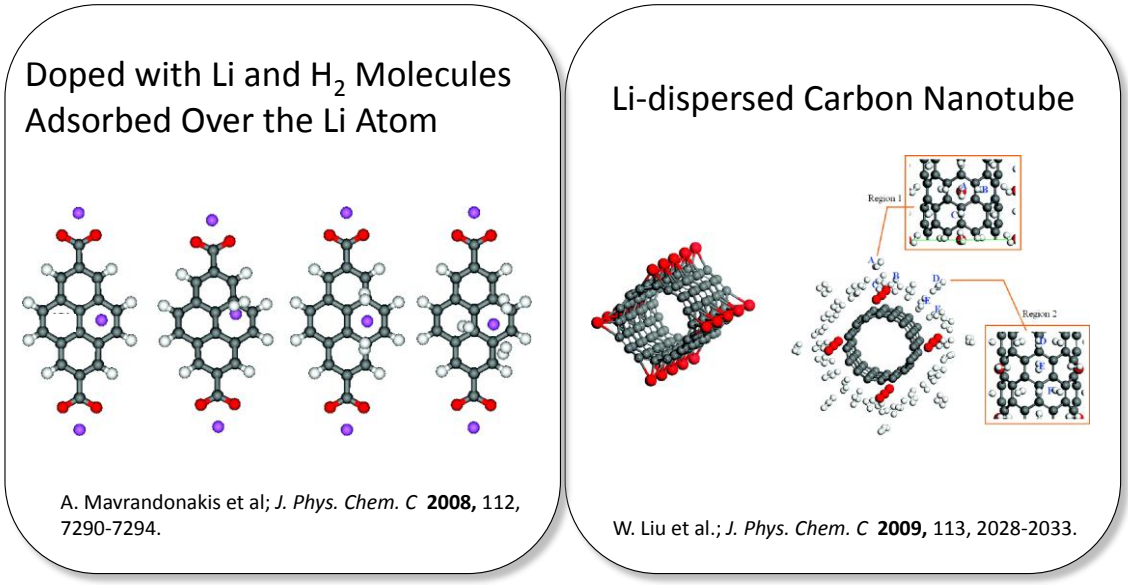

Figure 1.11. Calculation results of hydrogen adsorption of lithium doped carbon materials [31,32].

1.5 Purpose of this research

In this study, I aimed to obtain carbon materials with under 1 nm and heat of adsorption under 15 kJ/mol-H_2. These poroperties are expected to be hydrogen storage materials suitable for practical use around ambient temperatures and hydrogen tank pressure. The purpose is to develop a means of transporting hydrogen gas in a compact manner (Figure 1.12). If the 35 MPa hydrogen tank is filled with 5 mass% hydrogen storage materials, the total hydrogen mass quantity in the tank should increase to 1.6 times, compared with the amounts before filled with hydrogen storage materials.

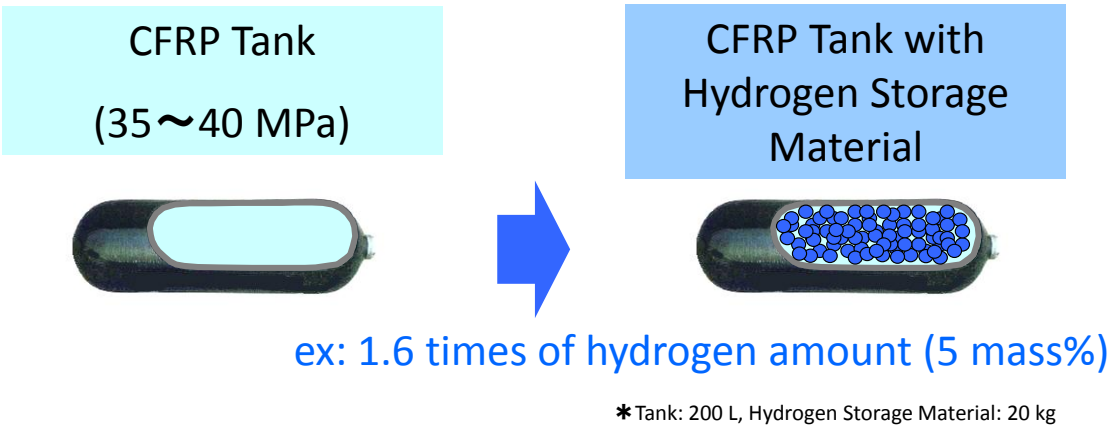

Figure 1.12. Hydrogen storage and transportation method.

In this thesis, hydrogen storage materials made from activated carbon have been studied. Activated carbons are low-cost, good hydrogen gas accessibility at around ambient temperatures. KOH activated carbons are synthesized that are supposed to have higher storage capacity at ambient temperatures. KOH activation makes higher surface area and bigger micropore volume. I have studied the hydrogen storage capacity of activated carbon species synthesized under various conditions of KOH activation treatment. Precursors of various origin, such as rice husk and PAN (Poly-acrylonitrile) fiber were used as the raw materials. The activated PAN fiber carbons have larger micropore volumes than the rice husk carbons.

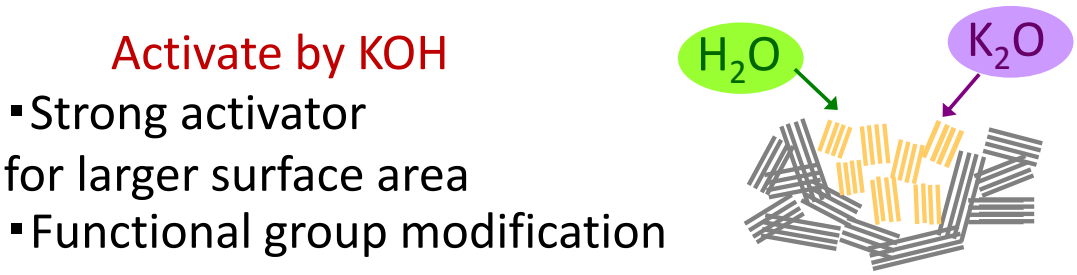

Figure 1.13. The effect and characteristics of KOH activation.

However these materials are needed to have higher heat of adsorption than ordinal carbon materials around 5 kJ/mol-H_2 to enhance hydrogen storage affinity. Therefore, I considered that the KOH activated carbons are ideal materials for lithium doping to develop novel hydrogen storage materials. Then, I focused on to lithium doping on the acidic surface functional groups of the activated carbons, because the acidic functional groups can easily react with basic reagent and exchange cations. But it has not yet reported lithium doped activated carbons with such acid-base reaction. By the acid-base reaction with basic lithium reagent, the oxygen containing functional groups will be introduced lithium.

The hydrogen adsorption performance of several types of lithium doped KOH activated carbons has also been studied.

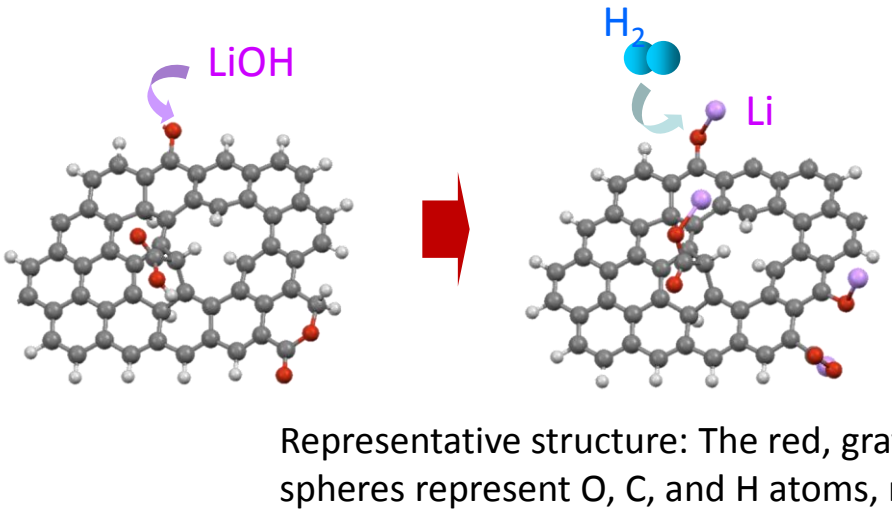

Figure 1.14. The schematic representation of Lithium doping by LiOH to the functional group of the surface of KOH activated carbons.

1.6 Reference

[1] A. Zuttel, A. Borgschulte, L. Schlapbach, *Hydrogen as a Future Energy Carrier*, **2008**, Wiley-VCH: Weinheim, Germany.
[2] P. Jena, Materials for hydrogen Storage; Past, Present, and Future, *J. Phys. Chem. Let.* **2011**, *2,* 206-211.
[3] W. L. Mao, C. A. Koh, E. D. Sloan, Clathrate Hydrates under Pressure. *Phys. Today* **2007**, *60*, 42–47.
[4] L. Schlapbach,; A. Zuttel, Hydrogen-Storage Materials for Mobile Applications. *Nature* **2001**, *414*, 353–358.
[5] A. Zuttel, Materials for hydrogen storage. *Materials Today*, **2003**, *6*, 24-33.
[6] M. A. de la Casa-Lillo, F. Lamari-Darkrim, D. Cazorla- Amorós, and A. Linares-Solano, Hydrogen Storage in Activated Carbons and Activated Carbon Fibers, *J. Phys. Chem. B*, **2002**, *106*, 10930-10934.
[7] H. Wang, Q. Gao, and J. Hu, High Hydrogen Storage Capacity of Porous Carbons Prepared by Using Activated Carbon, *J. Am. Chem. Soc.* **2009**, *131*, 7016–7022.
[8] K. M. Thomas, Hydrogen adsorption and storage on porous materials, *Catalysis Today*, **2007**, *120*, 389-398.
[9] M. G. Nijkamp, J. E. M. J. Raaymakers, A. J. van Dillen, K. P. de Jong , Hydrogen storage using physisorption - materials demands, *Appl. Phys. Lett. A*, **2001**, *72*, 619-623.
[10] H. Takagi, H. Hatori, Y. Soneda, N. Yoshizawa, Y. Yamada, Adsorptive hydrogen storage in carbon and porous materials, *Materials Science and Engineering: B*, **2004**, *108*, 143-147.
[11] A. K. Singh, J. Lu, R. S. Aga, B. I. Yakobson, Hydrogen Storage Capacity of Carbon-Foams: Grand Canonical Monte Carlo Simulations, *J. Phys. Chem. C*, **2011**, *115*, 2476–2482.
[12] A. D. Leonard, J. L. Hudson, H. Fan, R. Booker, L. J. Simpson, K. J. O'Neill, P. A. Parilla, M. J. Heben, M. Pasquali, C. Kittrell, J. M. Tour, Nanoengineered Carbon Scaffolds for Hydrogen Storage, *J. Am. Chem. Soc.* **2009**, *131*, 723–728.
[13] D. W. Boukhvalov and M. I. Katsnelson, Chemical Functionalization of Graphene with Defects, *Nano Letters,* **2008**, *8*, 4373-4379.
[14] G. Srinivas, Y. Zhu, R. Piner, N. Skipper, M. Ellerby, R. Ruoff, Synthesis

of graphene-like nanosheets and their hydrogen adsorption capacity, *Carbon*, **2010**, *48*, 630–635.
[15] F. D. Lamari, D. Levesque, Hydrogen adsorption on functionalized graphene, *Carbon*, **2011**, *49*, 5196–5200.
[16] Z. Ryu, H. Rong, J. Zheng, M. Wang, B. Zhang, Microstructure and chemical analysis of PAN-based activated carbon fibers prepared by different activation methods, *Carbon*, **2002**, *40*, 1131–1150.
[17] X. B. Zhao, B. Xiao, A. J. Fletcher, and K. M. Thomas, Hydrogen Adsorption on Functionalized Nanoporous Activated Carbons, *J. Phys. Chem. B*, **2005**, *109*, 8880-8888.
[18] S. Naganoa, H. Tamonb, T. Adzumib, K. Nakagawab, T. Suzukib, Activated carbon from municipal waste, Carbon, **2000**, *38*, 915–920.
[19] M. A. Lillo-Ródenas, D. Cazorla-Amorós, A. Linares-Solano, F. Béguin, C. Clinard, J.N. Rouzaud, HRTEM study of activated carbons prepared by alkali hydroxide activation of anthracite, *Carbon*, **2004**, *42*, 1305–1310.
[20] H. Benaddi, T. J. Bandosz, J. Jagiello, J. A. Schwarz, J. N. Rouzaud, D. Legras, F. Béguin, Surface functionality and porosity of activated carbons obtained from chemical activation of wood, *Carbon,* **2000**, *38*, 669–674.
[21] V. V. Bhat, C. I. Contescu, N. C. Gallego, F. S. Baker, Atypical hydrogen uptake on chemically-activated, ultramicroporous carbon, *Carbon*, **2010**, *48*, 1331–1340.
[22] N. Texier-Mandoki, J. Dentzer, T. Piquero, S. Saadallah, P. David, C. Vix-Guterl, Hydrogen storage in activated carbon materials: Role of the nanoporous texture, *Carbon*, **2004**, *42*, 2744–2747.
[23] S. Yoon, S. Lim, Y. Song, Y. Ota, W. Qiao, A. Tanaka, I. Mochida, KOH activation of carbon nanofibers, *Carbon*, **2004**, *42*, 1723–1729.
[24] M. Monteiro de Castro, M. Martínez-Escandell, M. Molina-Sabio, F. Rodríguez-Reinoso, Hydrogen adsorption on KOH activated carbons from mesophase pitch containing Si, B, Ti or Fe, *Carbon*, **2010**, *48*, 636–644.
[25] M. A. Lillo-Ródenas, D Cazorla-Amorós, A Linares-Solano, Understanding chemical reactions between carbons and NaOH and KOH: An insight into the chemical activation mechanism, *Carbon*, **2003,** *41*, 267–275.
[26] S. Park, W. Jung, Preparation of activated carbons derived from KOH-impregnated resin, Carbon, **2002**, *40*, 2021–2022.
[27] I. Martin-Gullon, J. P. Marco-Lozar, D. Cazorla-Amorós, A. Linares-Solano, Analysis of the microporosity shrinkage upon thermal

post-treatment of H_3PO_4 activated carbons, *Carbon*, **2004**, *42*, 1339-1343.
[28] I. Toda, H. Ono, T. Takahata, S. Ohshio, H. Akasaka, S. Himeno, T. Kokubu, H. Saitoh, Hydrogen Storage Property of Nanoporous Carbon Materials Prepared from Rice Husks, *J. Sol. Mech. Mat. Eng.* **2009**, *3*, 1306-1311.
[29] S. S. Han, W. A. Goddard, Lithium-Doped Metal-Organic Frameworks for Reversible H_2 Storage at Ambient Temperature, *J. Am. Chem. Soc.* **2007**, *129*, 8422-8423.
[30] H. Tachikawa, A. Shimizu, Diffusion Dynamics of the Li^+ Ion on a Model Surface of Amorphous Carbon: A Direct Molecular Orbital Dynamics Study. *J. Phys. Chem. B* **2005**, *109*, 13255-13262.
[31] A. Mavrandonakis, E. Tylianakis, A. K. Stubos, G. E. Froudakis, Why Li Doping in MOFs Enhances H_2 Storage Capacity? A Multi-scale Theoretical Study. *J. Phys. Chem. C* **2008**, *112*, 7290-7294.
[32] W. Liu, Y. H. Zhao, Y. Li, Q. Jiang, E. J. Lavernia, Enhanced Hydrogen Storage on Li-Dispersed Carb. *J. Phys. Chem. C* **2009**, *113*, 2028–2033
[33] H. Takagi, Analysis of surface structure of carbon materials by using temperature-programmed desorption method. *Tanso,* **2009**, *237*, 67-71.

Chapter 2

Hydrogen Storage by Activated Carbons Made from PAN(Poly-acrylonitrile)

Abstract

KOH activated carbon made from PAN(Poly-acrylonitrile) can adsorb large amount of hydrogen at an ambient temperature. Carbon species synthesized under various conditions of KOH activation treatment have different properties of adsorption and hydrogen storage capacities. KOH activated carbons from PAN have 2625-3145 m^2/g BET specific surface areas. Then, the micropore diameter is 0.9-1.5 nm. The highest highest hydrogen adsorption capacity for a KOH activated carbon from PAN is 1.1 mass% at 303 K/30 MPa. The synthesized materials show hydrogen storage capacities that are proportional to their BET specific surface areas and micropore volumes. At the same time, hydrogen storage capacity is also affected by micropore size of the under 2 nm; smaller micropores are preferable for hydrogen storage. The micropore sizes around 0.9-1.3 nm are more suitable for hydrogen storage at ambient temperatures.

2.1 Introduction

I tried to synthesize activated carbon as hydrogen storage materials with effective KOH activation treatment from PAN fibers because they have reached high BET surface area around 3000 m^2/g [1]. I have designed several sets of activation conditions and investigated porosity by way of adsorption measurements. Then, each material's hydrogen storage capacity was measured at 303 K. In addition, I studied the relationship between the porous properties details of the materials such as micropore volume and micropore size, and their hydrogen storage capacities at ambient temperature. The research reported in this paper is aimed to clarify and optimize which types of porous structures are favorable for increased hydrogen storage in practical conditions.

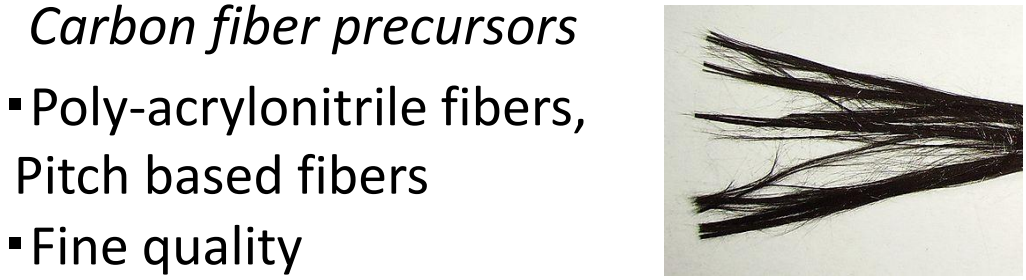

Figure 2.1. The characteristics of carbon fiber precursors.

2.2 Experimental section

2.2.1 Carbon materials

PAN fiber precursors were selected as the raw materials for the activated carbons. PAN fiber was usually made by several calcination processes. But the precursor did not have final calcination process. The activated carbon "PAN-A" was made using PAN fiber unwoven fabric. "PAN-B" was made using PAN fiber. Activation was performed using the chemical reagent KOH, under several sets of activation conditions (Synthesized by Environmental Technique Service Co.).

First, the raw materials were pre-calcined from room temperature to 773-973 K over 12 hrs in the furnace under nitrogen gas flowing. Then the sample was ball-milled to 10-20 μm. Next, KOH treatment was performed using a homogeneous mixture of KOH flake (thin slice of KOH tablet) and pre-calcined material, in a furnace heated to the activation temperature from room temperature to 1023 K under nitrogen over 7 hrs and kept 1023 K for 1-2 hrs. The amounts of KOH reagent used ranged from 3.2 to 4.5 times of the sample. The mixture was then stirred in water of 20 times volume of the sample, after which the activated carbon was filtered out and rinsed. The filtering/rinsing process was repeated several times. The activated carbon was then stirred in a 0.1 N hydrochloric acid solution of 20 times volume of the sample, after which it was again rinsed with water and filtered out repeatedly. Finally, the samples were dried by heating at 383 K and the porous carbon materials were obtained as black powder. The activation conditions are shown in Table 2.1. The pre-calcination temperatures ranged from 773 to 973 K, and the amounts of KOH reagent used ranged from 3.2 to 4.5 times that of the raw carbon materials.

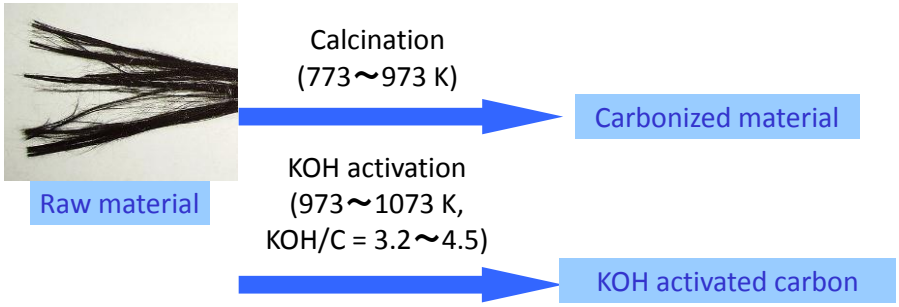

Scheme 2.1. The schematic representation of the manufacturing process of KOH activated carbons made from PAN.

2.2.2 Characterization

Elemental analysis was performed on the KOH-activated carbons. The analyzer used to measure C, H, and N was a Vario EL III by Elementar. The analyzer used to measure O was an EA1110 by CE Instruments.

The BET surface area and pore volume were estimated by measuring nitrogen adsorption at 77 K, using a BELSORP-max instrument. Before the measurement, the samples were dried under vacuum at 523 K for 4 hrs. Surface area was estimated by the Brunauer-Emmet-Teller (BET) method at a relative pressure around 0-0.25. Micropore volume was calculated using the Dubinin-Radushkevich (DR) method. Mesopore volume was calculated by subtracting the micropore volume from the total pore volume. Peak pore size was estimated using the MP method.

2.2.3 Hydrogen adsorption measurements

Hydrogen adsorption was measured by the volumetric method (hydrogen storage capacity measuring apparatus by Fuse Technonet Co., LTD). Before the measurement, the samples were dried under vacuum at 523 K for 4 hrs. In the pressure vessel the sample was degassed and was maintained at 303 K. After closing the valve connected to the pressure vessel, the pressure in the hydrogen reservoir was controlled for introducing hydrogen. After closing the pressure vessel, the equilibrium pressure was obtained in the hydrogen reservoir and sample cell. The stored hydrogen content in the sample was calculated from the pressure drop measured by pressure gauge. The stored contents were expressed as weight ration of hydrogen (mass%) on total weight. Measurements were performed under various pressures: 0-12 MPa or 0-35 MPa at 303 K, and 0-1 MPa at 77 K.

2.3 Results and discussion

2.3.1 Elemental analysis

Elemental analyses for C, H, and N were conducted. The KOH-activated PAN carbon "PAN-A" contained 75% C and 10% N, which indicated that the CN groups had not been completely removed in the activation process. "PAN-B" showed a different composition: 77-95% C, 1-6% N and 4-16% O. Differences in their elemental compositions were found depending on the activation conditions.

2.3.2 Pore volume and pore size estimation

The nitrogen adsorption-desorption isotherms for the KOH-activated carbons are shown in Figure 2.2. These activated carbons adsorbed nitrogen at low relative pressure, which indicated that these materials had well developed micropores. The activated PAN-A carbons showed Type-I isotherms, while the PAN-B carbons showed mixed Type-I+IV isotherms [2]. The characteristic feature of a Type-I isotherm is a long horizontal plateau, which extends up to relatively high P/P_0. Pores are typically microporus with the exposed surface residing almost exclusively inside the microspores, which once filled with adsorbate, leave little or no external surface for further adsorption. Type-IV occurs on porous adsorbents with pores in the range of 1.5-100 nm. At higher pressures the slope shows increased uptake of adsorbate as pores become filled, inflection point typically occurs near completion of the first monolayer.

The micropore and mesopore volumes varied, depending on the activation conditions. The adsorption properties of the materials are shown in Table 1. The activated PAN-A carbons had smaller pore volumes (micropore volume of 0.9-1.0 cm^3/g and mesopore volume of 0.05 cm^3/g) compared to the activated carbons obtained from the other raw materials. In contrast, the PAN-B carbons had much greater micropore and also mesopore volumes. For the PAN-B carbons, micropore volumes ranged from 1.2 to 1.7 cm^3/g and mesopore volumes ranged from 0.2 to 1.2 cm^3/g. Among the PAN-B carbons, those calcined at higher temperatures showed more developed porosity, in terms of both micropore and mesopore volume. Also, the larger the amount of KOH reagent that was added for activation, the greater the volumes of micropores and mesopores that were formed. Hydrogen was adsorbed mainly

in the micropores, and mesopores were found to be less effective for hydrogen storage. The results of micropore size analysis (by the MP method) of the PAN-B carbons are shown in Table 2.1. I made a detailed study of the micropore properties of PAN-B, based on the micropore size analysis. The results indicate that when the material was calcined at 873 K, using a higher proportion of KOH to the raw carbon material resulted in a larger range of pore sizes. Furthermore, the higher the calcination temperature became, the more uniform the pore size distribution. When the material was calcined at 973 K, using a higher proportion of KOH to the raw carbon material resulted in larger pore sizes, but the range was kept tighter (Figure 2.3-2.6). The mesopore volume depended on the amount of KOH added. For example, when KOH was added to the raw carbon material at a ratio of four and a half parts to one, a larger number of mesopores formed.

Table 2.1. Activation conditions of PAN carbons and nitrogen adsorption measurement results.

Raw material	Sample	Temp.[a], K	KOH quantity[b]	S_{BET}[c], m^2/g	V_t[d], cm^3/g	V_{micro}[e], cm^3/g	V_{meso}[f], cm^3/g	d_P[g], nm
PAN-A	PAN-A1	773	3.5	1597	0.92	0.87	0.05	
	PAN-A2	873	3.7	1747	1.05	1.00	0.05	
PAN-B	PAN-B1	873	3.2	2625	1.44	1.24	0.21	0.9
	PAN-B2	873	3.8	2778	1.84	1.30	0.54	1.3
	PAN-B3	973	3.8	3029	2.03	1.37	0.67	1.2
	PAN-B4	973	4.5	3145	2.90	1.73	1.17	1.5

[a] Calcination temperature in pre-calcination process. [b] Amount of KOH reagent added to the carbon raw material, expressed as a ratio of X:1. [c] Surface area (S_{BET}) was estimated by the Brunauer-Emmet-Teller (BET) method at a relative pressure around 0-0.25. [d] V_t shows the total pore volume. [e] Micropore volume (V_{micro}) was calculated using the Dubinin-Radushkevich (DR) method. [f] Mesopore volume was calculated by subtracting the micropore volume from the total pore volume. [g] Peak pore size (d_P) was estimated using the MP method.

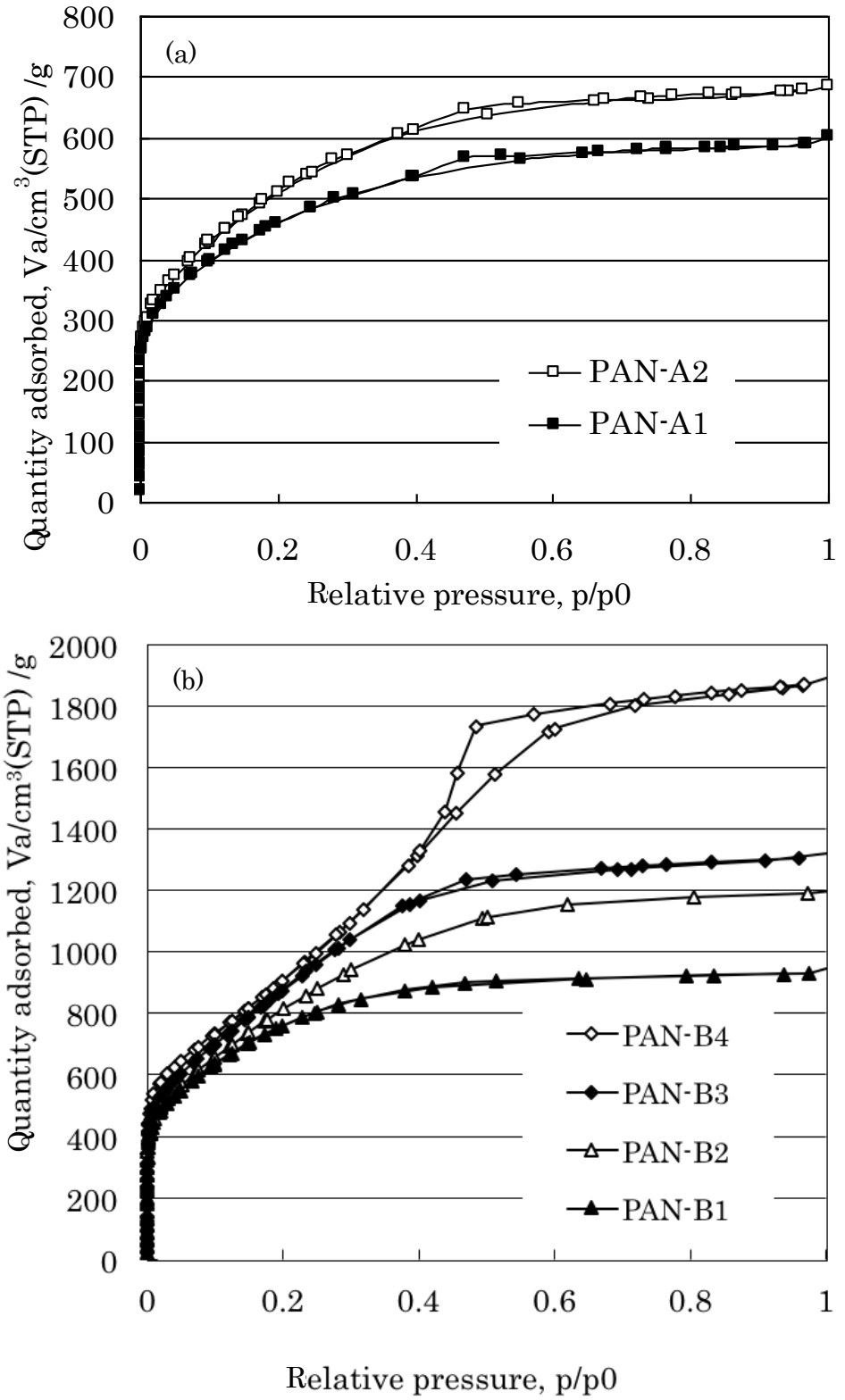

Figure 2.2. Nitrogen adsorption-desorption isotherms of KOH activated carbons from PAN-A (a) and PAN-B (b).

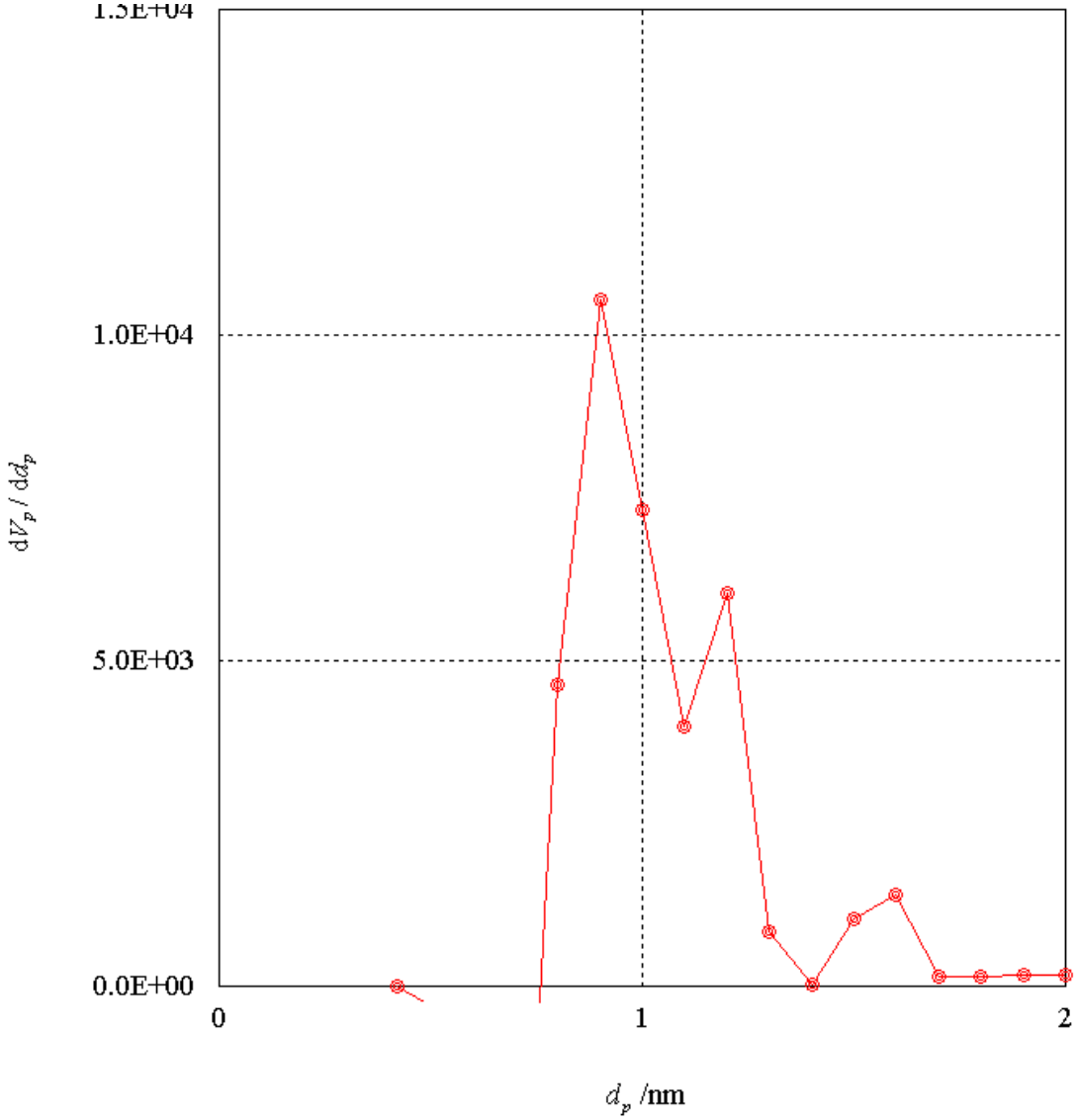

Figure 2.3. MP-plot of KOH activated PAN B-1 carbon.

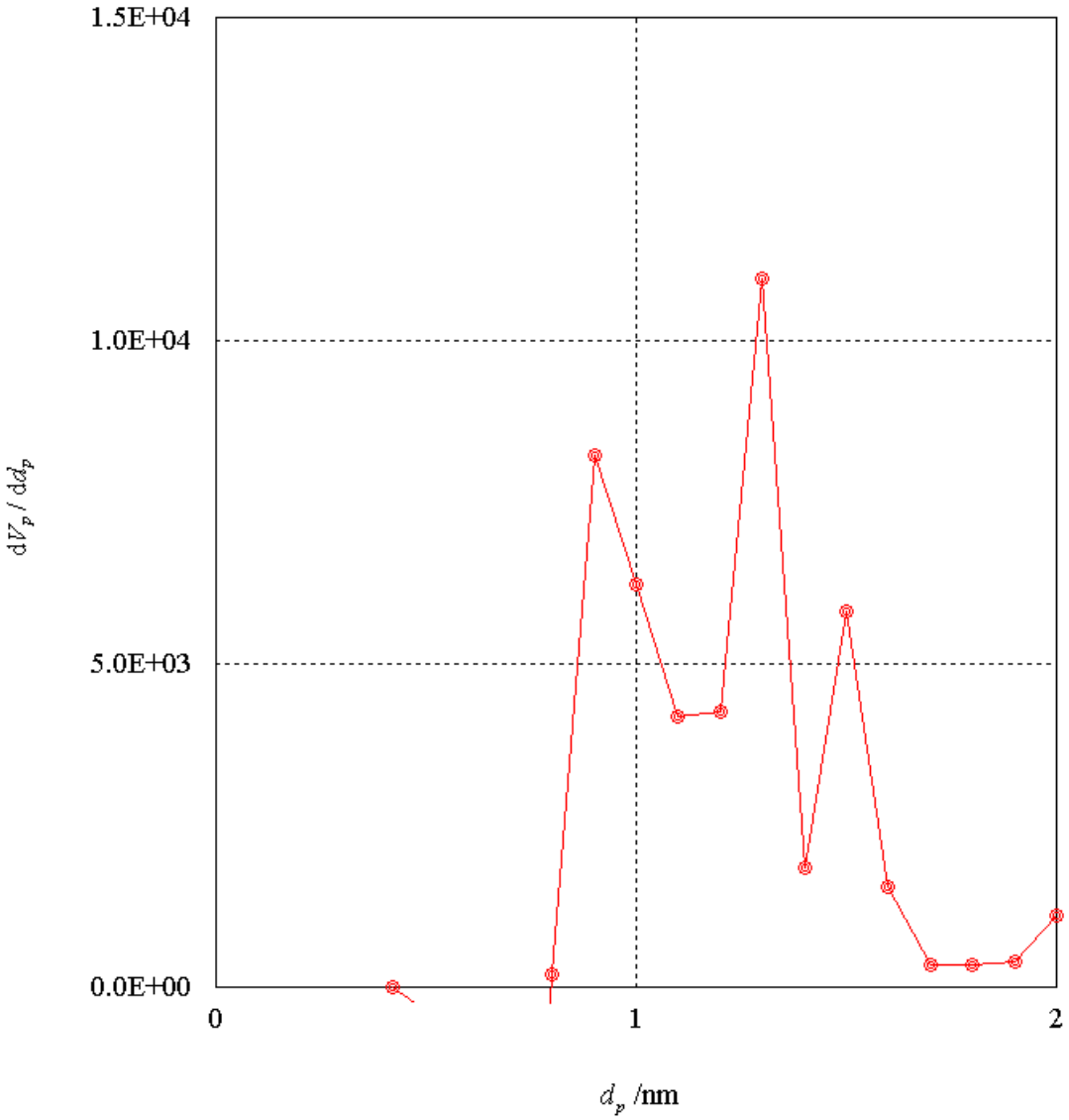

Figure 2.4. MP-plot of KOH activated PAN B-2 carbon.

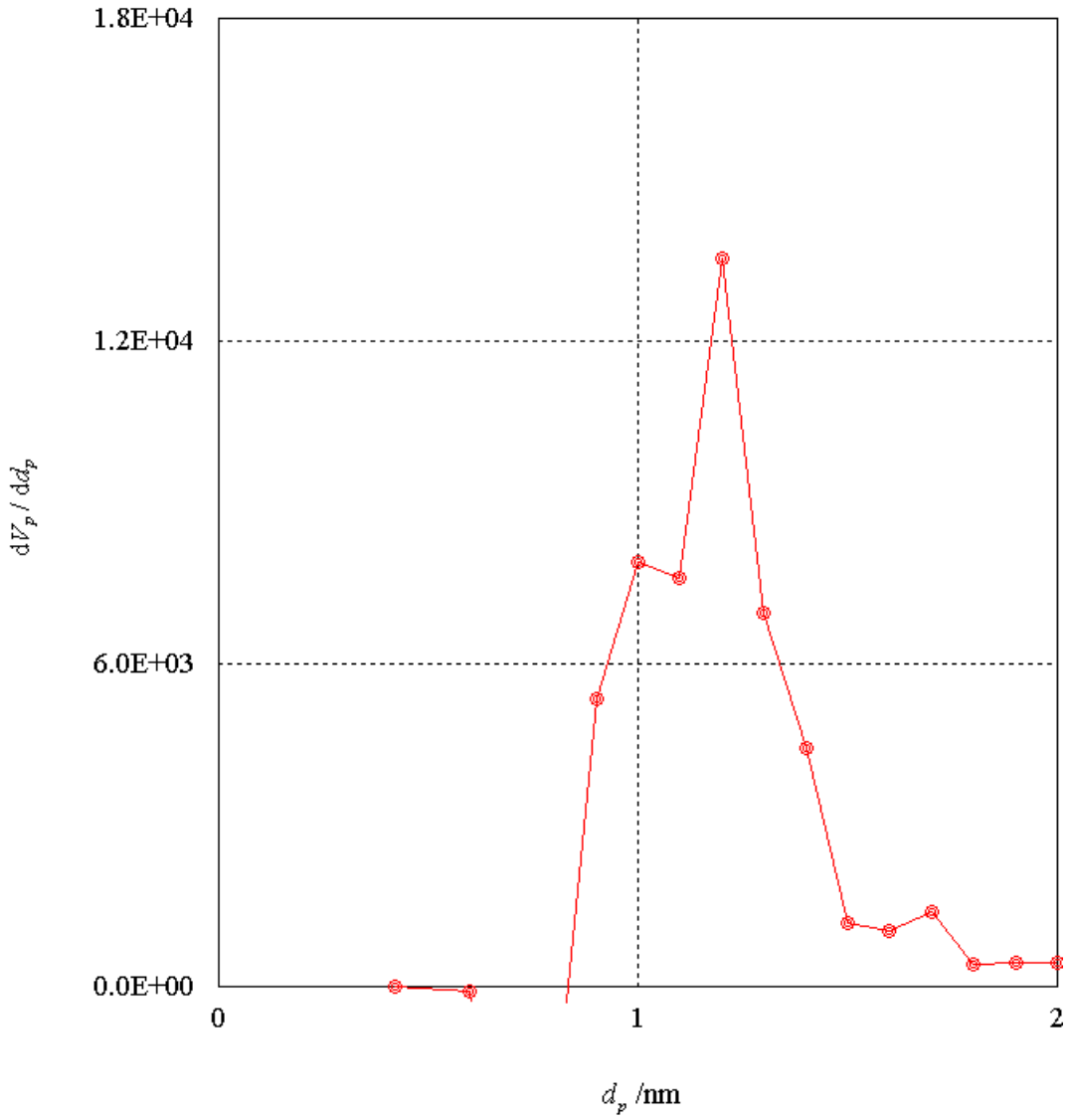

Figure 2.5. MP-plot of KOH activated PAN B-3 carbon.

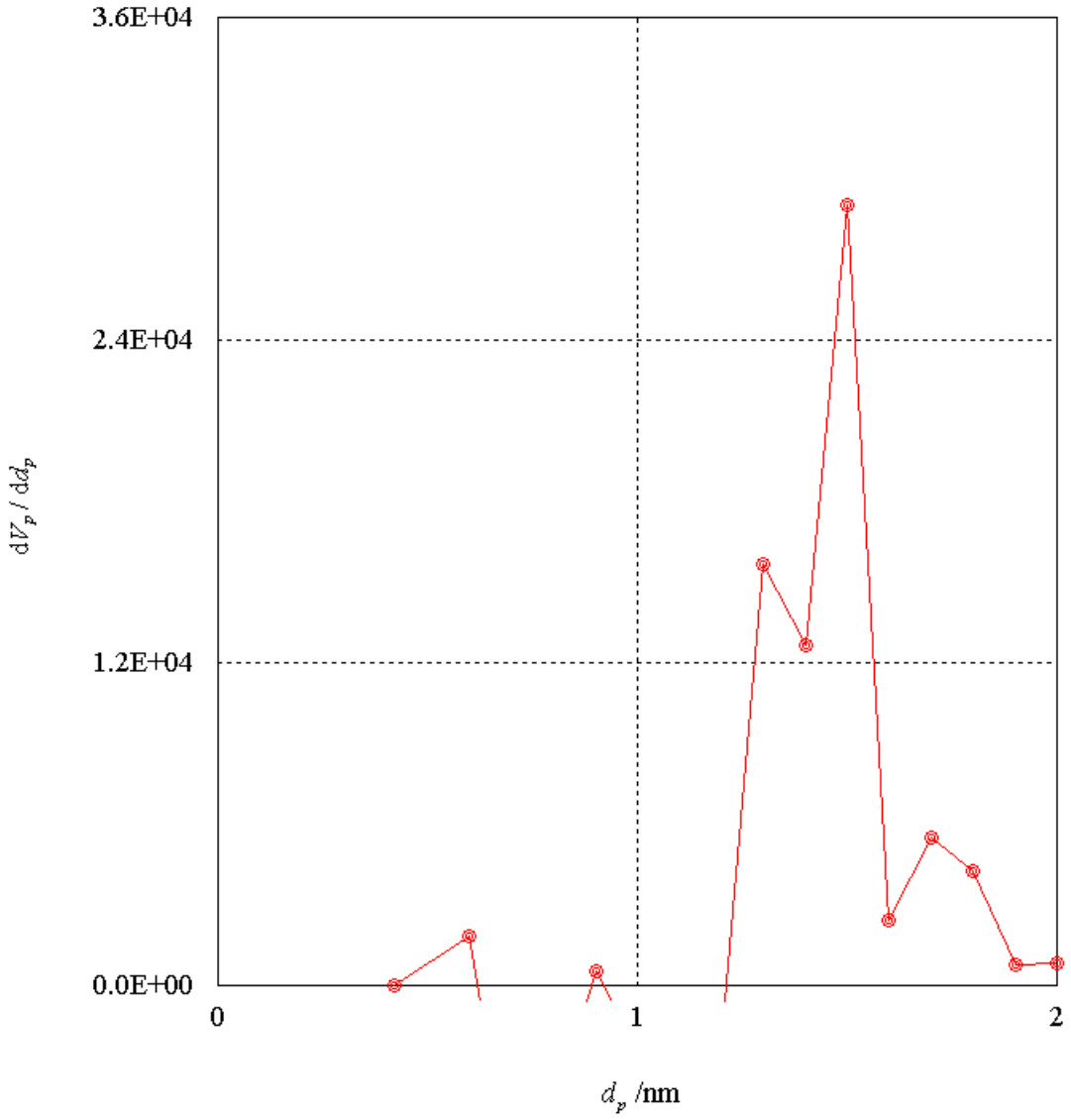

Figure 2.6. MP-plot of KOH activated PAN B-4 carbon.

2.3.3 Hydrogen adsorption

Hydrogen storage measurements were conducted on activated carbons synthesized under the conditions described above. Measurements were conducted at a temperature of 303 K and pressure ranges of 0-10 MPa and for PAN-B2 sample, 0-35 MPa. For PAN-B4 sample, hydrogen storage capacity was measured at 77 K/0-1 MPa. Hydrogen adsorption isotherms for the KOH activated carbons are shown in Figure 2.7 and hydrogen uptakes are shown in Table 2.2.

Table 2.2. Hydrogen storage properties of activated PAN carbons.

Sample	V_{micro} [a], cm^3/g	Hydrogen uptake (303 K)[b], mass%	Hydrogen uptake (303 K)[c], mass%	Hydrogen uptake (77 K)[d], mass%
PAN-A1	0.87	0.461		
PAN-A2	1.00	0.518		
PAN-B1	1.24	0.577		
PAN-B2	1.30	0.649	1.1 (30 MPa)	
PAN-B3	1.37	0.678		
PAN-B4	1.73	0.700		4.7

[a] Micropore volume (V_{micro}) was calculated using the Dubinin-Radushkevich (DR) method. [b] Hydrogen uptake at 303 K, 10 MPa. [c] Hydrogen uptake at 303 K, around 30 MPa. [d] Hydrogen uptake amount at 77 K, 0.7 MPa.

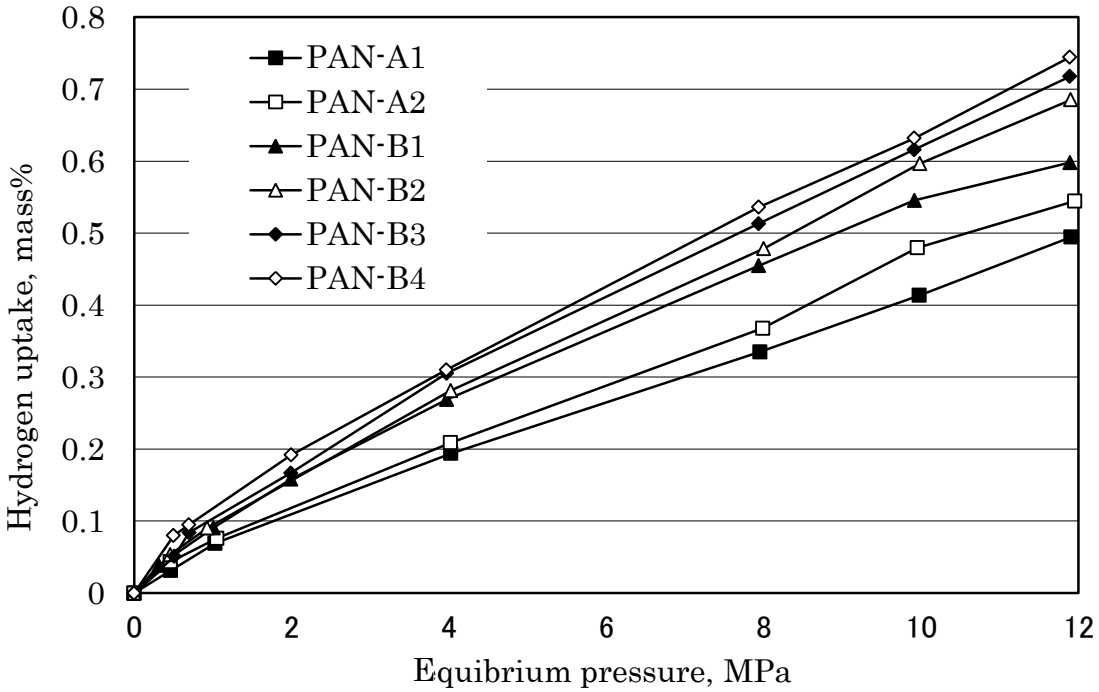

Figure 2.7. Hydrogen adsorption isotherms of KOH activated carbons from PAN at 303 K.

PAN-B carbons showed higher hydrogen storage capacities than the PAN-A carbons, depending on their activation conditions. Then, I looked at the relationship between hydrogen storage property and porosity. Figure 2.8(a) shows the relation between BET surface area and hydrogen uptake. Figure 2.8(b) shows the relation between micropore volume. In almost all the materials, hydrogen storage capacity was directly proportional to the not only BET surface area but also micropore volume. PAN-B4, which had the largest micropore volume, showed a lower hydrogen storage capacity than expected. This was because when PAN-B was calcined at 973 K and treated with KOH at a ratio of 4.5 parts to 1, the maximum micropore size was 1.5 nm. This micropore size was too large for hydrogen storage in room temperature. As a result, micropores of around 0.9-1.3 nm are suitable for hydrogen storage [2-4].

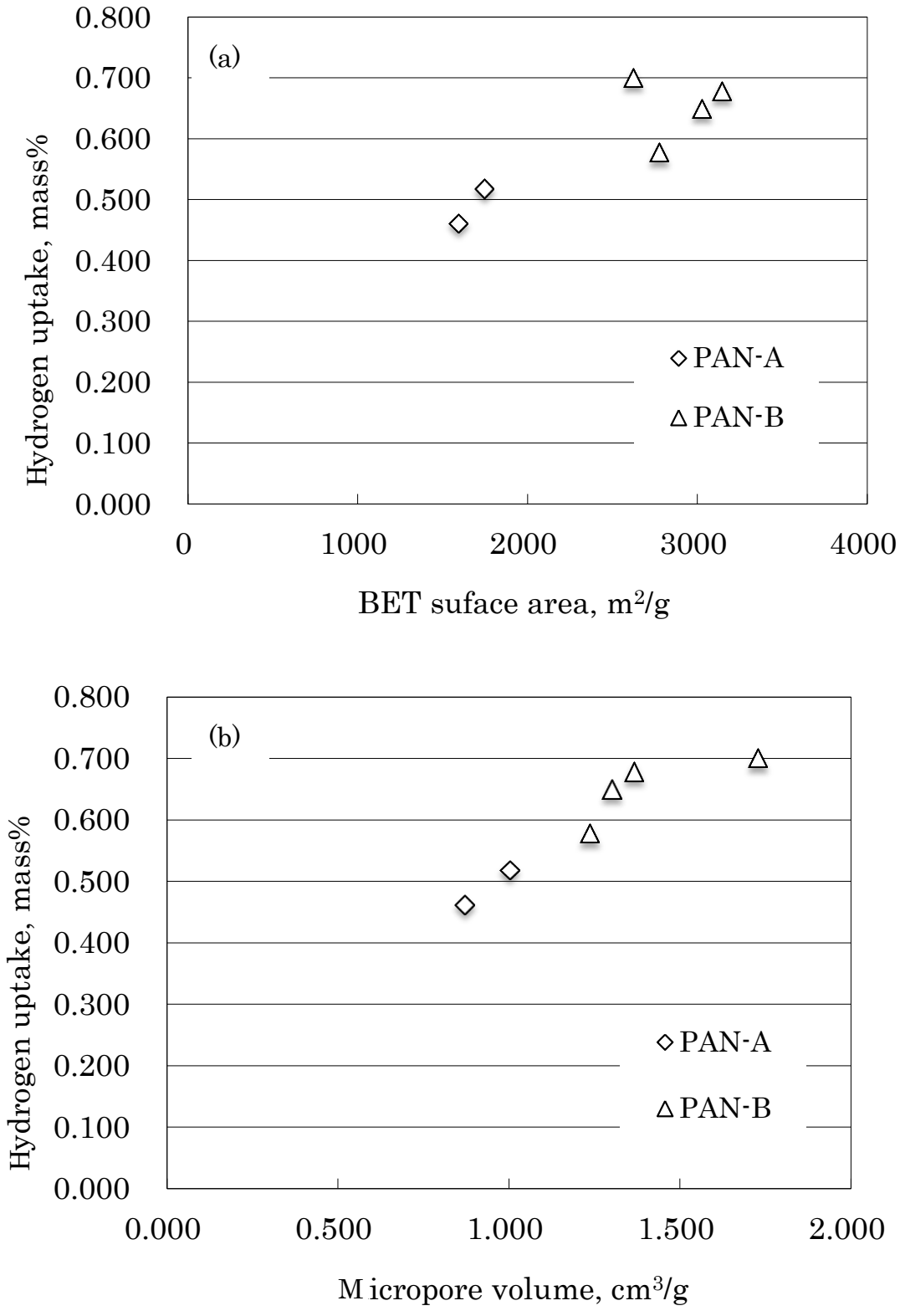

Figure 2.8. Hydrogen uptake vs. micropore volume (at 303 K, 10 MPa).

2.4 Conclusion

Several KOH activated carbons made from PAN were synthesized. Their porosity characteristics details and hydrogen adsorption capacities were measured. Activation under more severe conditions, i.e. higher amounts of KOH and/or higher pre-calcination temperatures, resulted in bigger micropore. Then bigger micropores translated to higher hydrogen adsorption uptake. However, with the activated PAN fiber carbons, it was shown that smaller micropore size is preferable for hydrogen adsorption at room temperature. The micropore sizes around 0.9-1.3 nm is more suitable for hydrogen storage at ambient temperatures.

2.5 Reference

[1] Z. Ryu, H. Rong, J. Zheng, M. Wang, B. Zhang, Microstructure and chemical analysis of PAN-based activated carbon fibers prepared by different activation methods, *Carbon*, **2002**, *40*, 1131–1150.
[2] H. Wang, Q. Gao, and J. Hu, High Hydrogen Storage Capacity of Porous Carbons Prepared by Using Activated Carbon, *J. Am. Chem. Soc*. **2009**, *131*, 7016–7022.
[3] I. Martin-Gullon, J. P. Marco-Lozar, D. Cazorla-Amorós, A. Linares-Solano, Analysis of the microporosity shrinkage upon thermal post-treatment of H_3PO_4 activated carbons, *Carbon*, **2004**, *42*, 1339-1343.
[4] I. Toda, H. Ono, T. Takahata, S. Ohshio, H. Akasaka, S. Himeno, T. Kokubu, H. Saitoh, Hydrogen Storage Property of Nanoporous Carbon Materials Prepared from Rice Husks, *J. Sol. Mech. Mat. Eng.* **2009**, *3*, 1306-1311.

Chapter 3

Hydrogen Storage by Activated Carbon Made from Rice Husk

Abstract

Rice husk are easily available a lot and low-cost. KOH activated carbons made from rice husk show high hydrogen storage capacity. Activated carbon species synthesized under various conditions of KOH activation treatment. KOH activated carbons from rice husk have 2052-2537 m^2/g BET specific surface areas. KOH activated carbons from rice husk have 0.9 nm micropore diameter, relatively high hydrogen storage density than KOH activated carbon made from PAN. The highest hydrogen adsorption capacity for a KOH activated carbon from rice husk carbon is 1.0 mass% at 303 K/27 MPa. The synthesized materials show hydrogen storage capacities that are proportional to their BET specific surface areas and micropore volumes. The micropore size was 0.9 nm uniformly and suitable for hydrogen storage at ambient temperatures.

3.1 Introduction

I tried to synthesize activated carbon for hydrogen storage materials with effective KOH activation treatment from rice husks because they could have reached high BET surface area around 3000 m^2/g [1]. I have designed several sets of activation conditions and investigated porosity by way of adsorption measurements. Then, each material's hydrogen storage capacity was measured at 303 K. In addition, I studied the relationship between the porous properties and their hydrogen storage capacities at ambient temperature. I examined the details of porous properties of the materials such as micropore volume and micropore size. The research reported in this paper is aimed to clarify and optimize which types of porous structures are favorable for increased hydrogen storage in practical conditions.

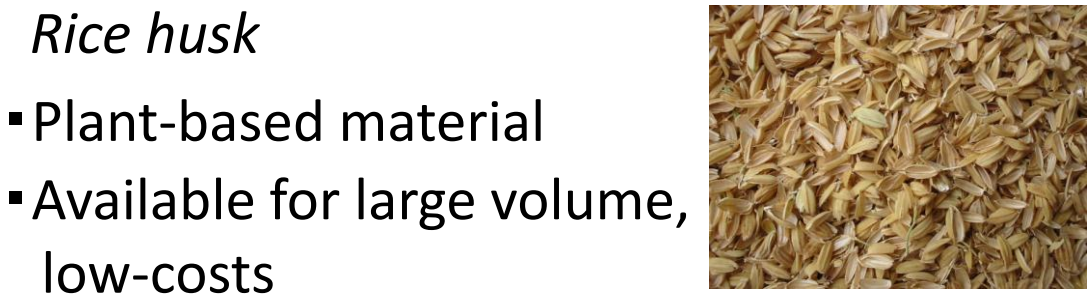

Figure 3.1. The characteristics of rice husks.

3.2 Experimental section

3.2.1 Carbon materials

Rice husk were selected as the raw materials for the activated carbons. The activated rice husk carbon was made from rice husk obtained from rice called "Yumetsukushi-mai" in Fukuoka, Japan. Activation was performed using the chemical reagent KOH, under two activation conditions (Synthesized by Environmental Technique Service Co.).

First, the raw materials were pre-calcined in the furnace from room temperature to 773 K or 973 K over 8 hrs. In the cooling time, nitrogen gas was flowed. Then silicate removal process was conducted. KOH was added to the pre-calcined sample in a furnace and heated at 1073 K for 2 hrs. Then the silicate removed sample was washed with water. The sample was dried then KOH treatment was performed using a homogeneous mixture of KOH flake (thin slice of KOH tablet) and silicate removed material, in a furnace heated from room temperature to the activation temperature 1023 K over 7 hrs under nitrogen and kept 1023 K for 1-2 hrs. The amount of KOH flake was ranged 3-4 times of the sample. The mixture was then stirred in water of 20 times volume of the sample, after which the activated carbon was filtered out and rinsed. The filtering/rinsing process was repeated several times. The activated carbon was then stirred in a 0.1 N hydrochloric acid solution of 20 times volume of the sample, after which it was again rinsed with water and filtered out repeatedly until pH became over 3. Finally, the samples were dried by heating at 383 K and ball-milled to 10-20 μm, the porous carbon materials were obtained as black powder. The activation conditions are shown in Table 3.1. The pre-calcination temperatures and the amounts of KOH reagent used are 773 K and 3.0 times that of the raw carbon materials and 973 K and 4.0 times that of the raw carbon materials.

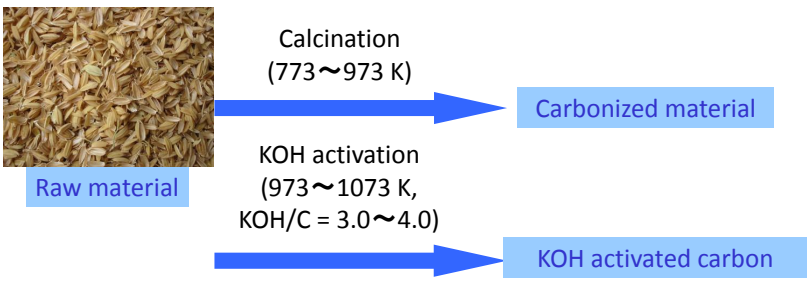

Scheme 3.1. The schematic representation of the manufacturing process of KOH activated carbons from rice husk.

3.2.2 Characterization

Elemental analysis was performed on the KOH activated carbons. The analyzer used to measure C, H, and N was a Vario EL III by Elementar. The analyzer used to measure O was an EA1110 by CE Instruments.

The BET surface area and pore volume were estimated by measuring nitrogen adsorption at 77 K, using a BELSORP-max instrument. Before the measurement, the samples were dried under vacuum at 523 K for 4 hrs. Surface area was estimated by the Brunauer-Emmet-Teller (BET) method at a relative pressure around 0-0.25. Micropore volume was calculated using the Dubinin-Radushkevich (DR) method. Mesopore volume was calculated by subtracting the micropore volume from the total pore volume. Peak pore size was estimated using the MP method.

3.2.3 Hydrogen adsorption measurements

Hydrogen adsorption was measured by the volumetric method (hydrogen storage capacity measuring apparatus by Fuse Technonet Co., LTD). Before the measurement, the samples were dried under vacuum at 523 K for 4 hrs. In the pressure vessel the sample was degassed and was maintained at 303 K. After closing the valve connected to the pressure vessel, the pressure in the hydrogen reservoir was controlled for introducing hydrogen. After closing the pressure vessel, the equilibrium pressure was obtained in the hydrogen reservoir and sample cell. The stored hydrogen content in the sample was calculated from the pressure drop measured by pressure gauge. The stored contents were expressed as weight ration of hydrogen (mass%) on total weight. Measurements were performed under various pressures: 0-12 MPa or 0-35 MPa at 303 K, and 0-1 MPa at 77 K.

3.3 Results and discussion

3.3.1 Elemental analysis

Elemental analyses for C, H, and N were conducted. The KOH activated carbons made from rice husk contained 82-85% C and 11-16% O. Compared to the activated PAN carbons, the rice husk carbons contained more O and less N.

3.3.2 Pore volume and pore size estimation

The nitrogen adsorption-desorption isotherms for the KOH activated carbons are shown in Figure 3.2. These activated carbons adsorbed nitrogen at low relative pressure, which indicated that these materials had well developed micropores. The rice husk carbons showed Type-I isotherms [2]. Type-I isotherm is a long horizontal plateau, which extends up to relatively high P/P_0. With the activated rice husk carbons, higher volumes of micropores and lower volumes of mesopores had formed, as compared to the PAN carbons. The mesopore volume depended on the amount of KOH added. For example, when KOH was added to the raw carbon material at a ratio of four parts to one, a larger number of mesopores formed. The calcination temperature had little effect on the total pore volume, but when calcinated at higher temperatures, the micropore volume decreased. The results of micropore size analysis of the rice husk carbons by the MP method are shown in Table 3.1. Changing the calcination temperature and amount of KOH had little effect on the pore size distribution (Figure 3.3-3.4).

Table 3.1. Activation conditions of rice husk carbons and nitrogen adsorption measurement results.

Raw material	Sample	Temp.[a], K	KOH quantity[b]	S_{BET}[c], m^2/g	V_t[d], cm^3/g	V_{micro}[e], cm^3/g	V_{meso}[f], cm^3/g	d_P[g], nm
Rice husk	Rice husk-1	773	3.0	2537	1.31	1.29	0.02	0.9
	Rice husk-2	973	4.0	2052	1.11	0.96	0.15	0.9

[a] Calcination temperature in pre-calcination process. [b] Amount of KOH reagent added to the carbon raw material, expressed as a ratio of X:1. [c] Surface area (S_{BET}) was estimated by the Brunauer-Emmet-Teller (BET) method at a relative pressure around 0-0.25. [d] V_t shows the total pore volume. [e] Micropore volume (V_{micro}) was calculated using the Dubinin-Radushkevich (DR) method. [f] Mesopore volume was calculated by subtracting the micropore volume from the total pore volume. [g] Peak pore size (d_P) was estimated using the MP method.

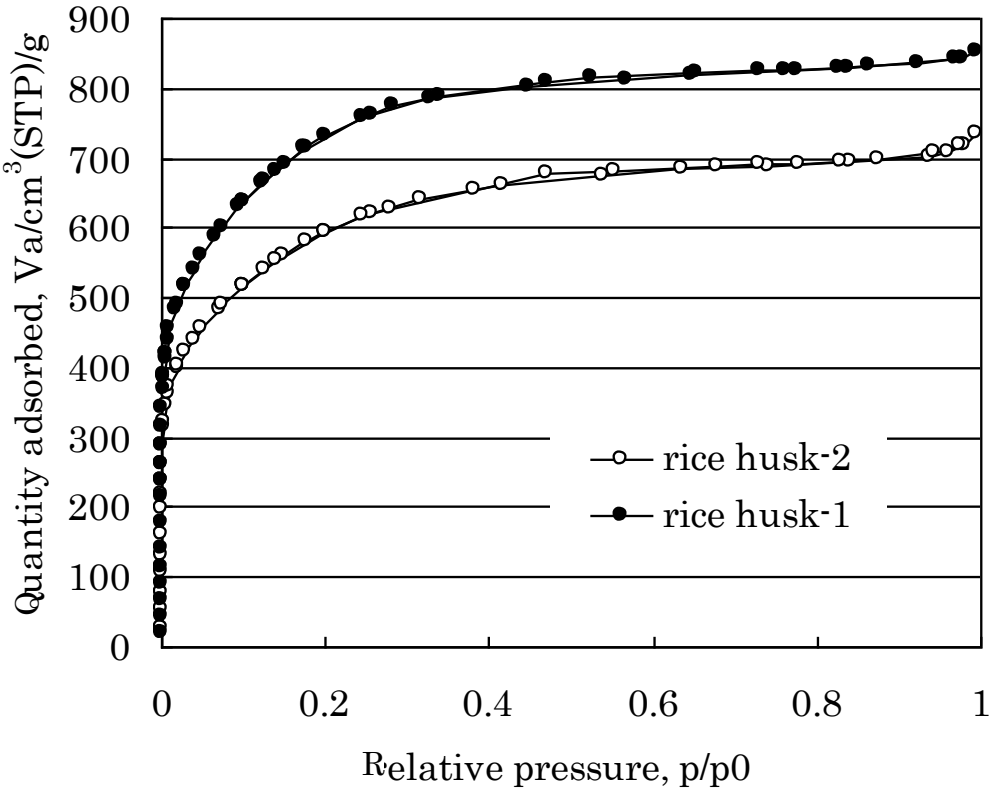

Figure 3.2. Nitrogen adsorption-desorption isotherms of KOH activated carbons from rice husk.

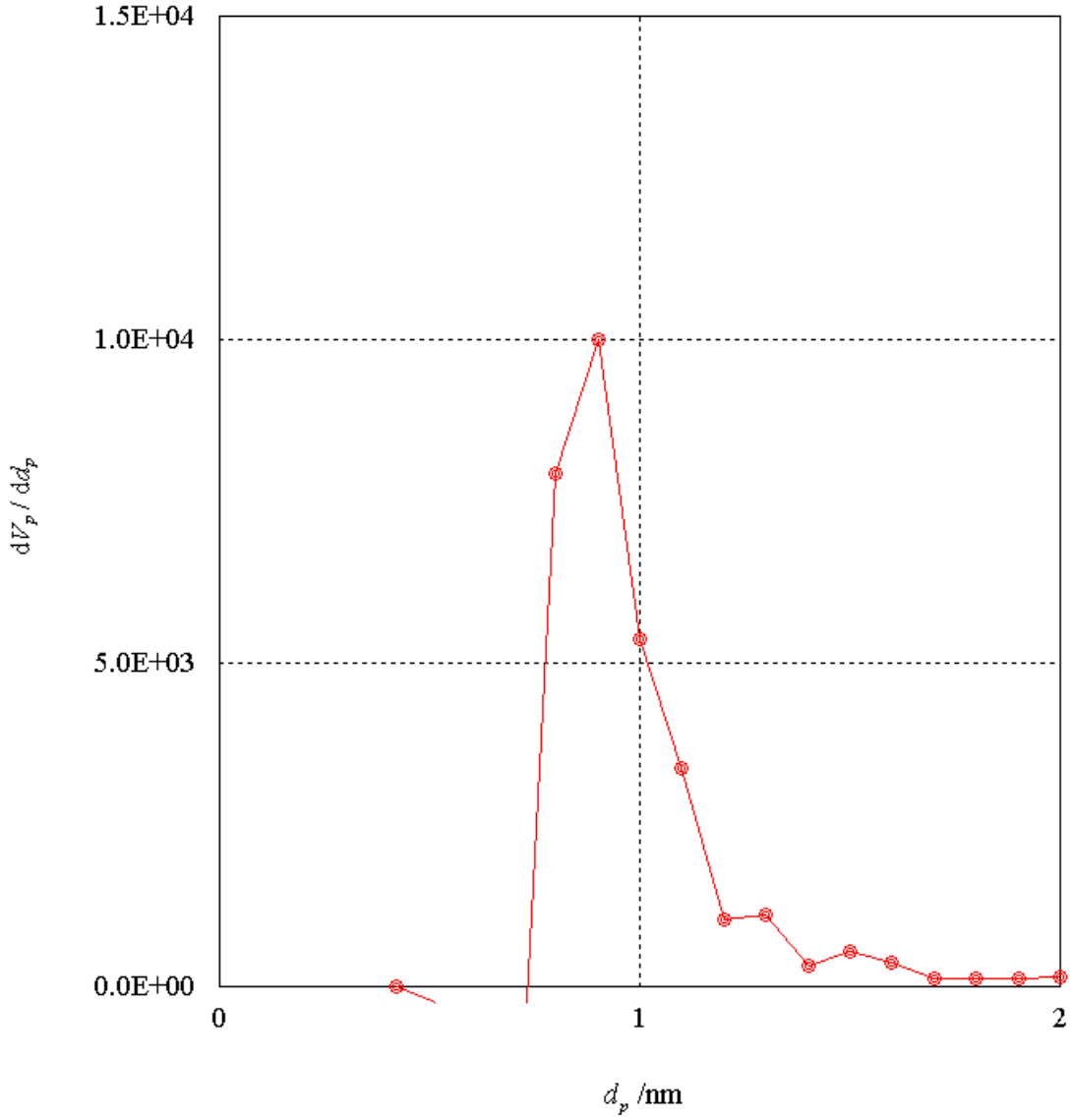

Figure 3.3. MP-plot of KOH activated rice husk-1 carbon.

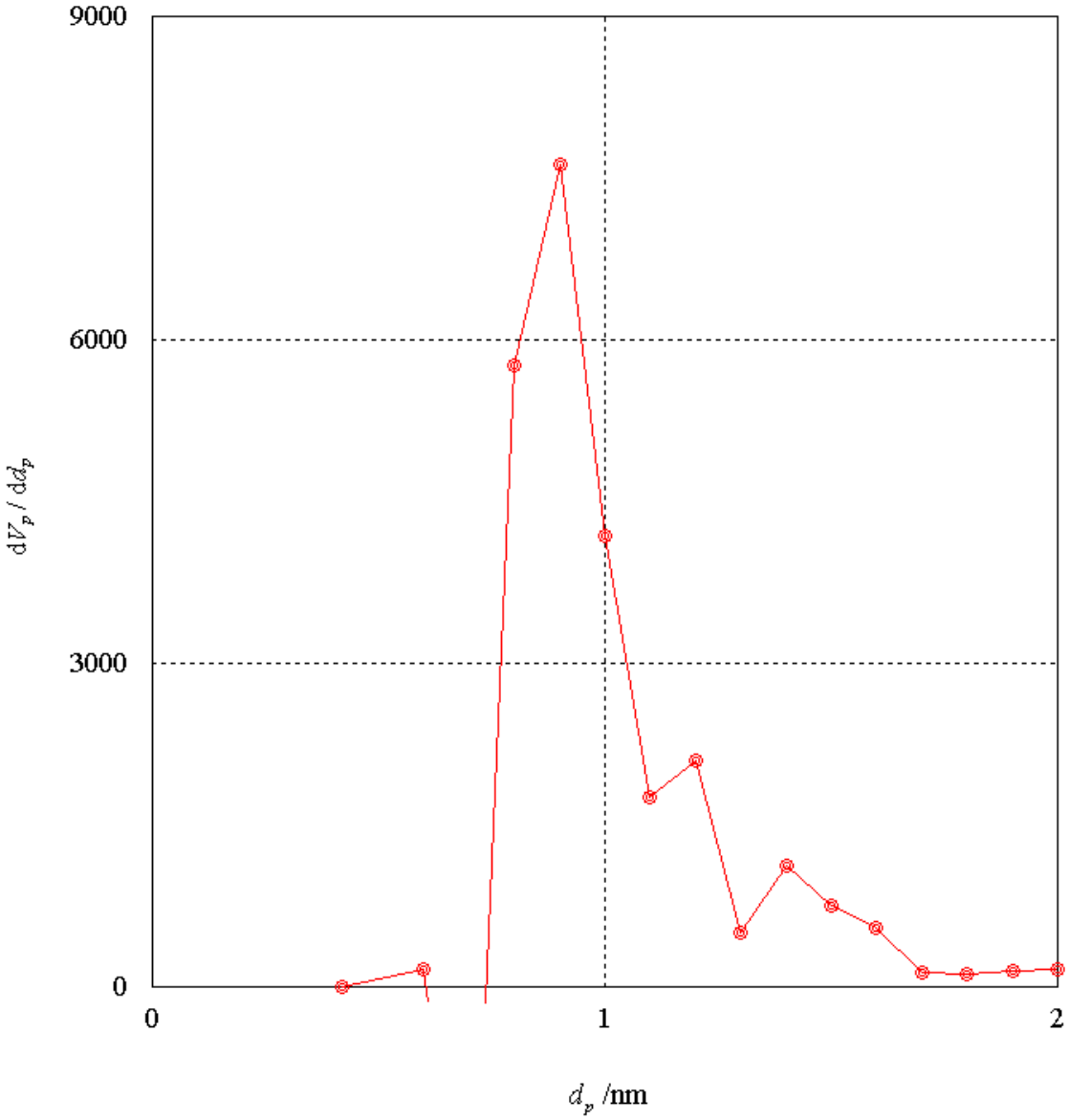

Figure 3.4. MP-plot of KOH activated rice husk-2 carbon.

3.3.3 Hydrogen adsorption

Hydrogen storage measurements were conducted on activated carbons synthesized under the conditions described above. Measurements were conducted at a temperature of 303 K and pressure ranges of 0-10 MPa and for rice husk-1sample, 0-35 MPa. For rice husk-1 sample, hydrogen storage capacity was measured at 77 K/0-1 MPa. Hydrogen adsorption isotherms for the KOH activated carbons are shown in Figure 3.5 and hydrogen uptakes are shown in Table 3.2.

Table 3.2. Hydrogen storage properties of activated riche husk carbons.

Sample	V_{micro} [a], cm^3/g	Hydrogen uptake (303 K)[b], mass%	Hydrogen uptake (303 K)[c], mass%	Hydrogen uptake (77 K)[d], mass%
Rice husk-1	1.29	0.712	1.0 (27 MPa)	4.1
Rice husk-2	0.96	0.460		

[a] Micropore volume (V_{micro}) was calculated using the Dubinin-Radushkevich (DR) method. [b] Hydrogen uptake at 303 K, 10 MPa. [c] Hydrogen uptake at 303 K, around 27 MPa. [d] Hydrogen uptake amount at 77 K, 0.7 MPa.

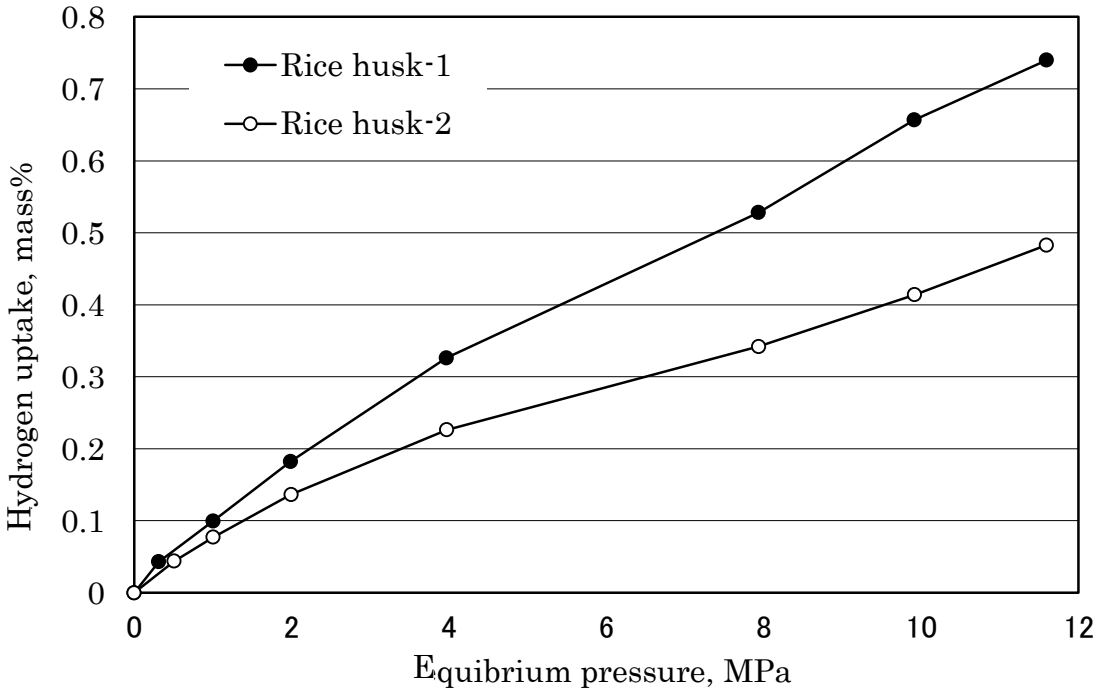

Figure 3.5. Hydrogen adsorption isotherms of KOH activated carbons from rice husk carbons at 303 K.

Then, I looked at the relationship between hydrogen storage property and porosity. Figure 3.6(a) shows the relation between BET surface area and hydrogen uptake. Figure 3.6(b) shows the relation between micropore volume. Hydrogen storage capacity was increased related to the not only BET surface area but also micropore volume. The micropores of around 0.9 nm are suitable for hydrogen storage [2-4].

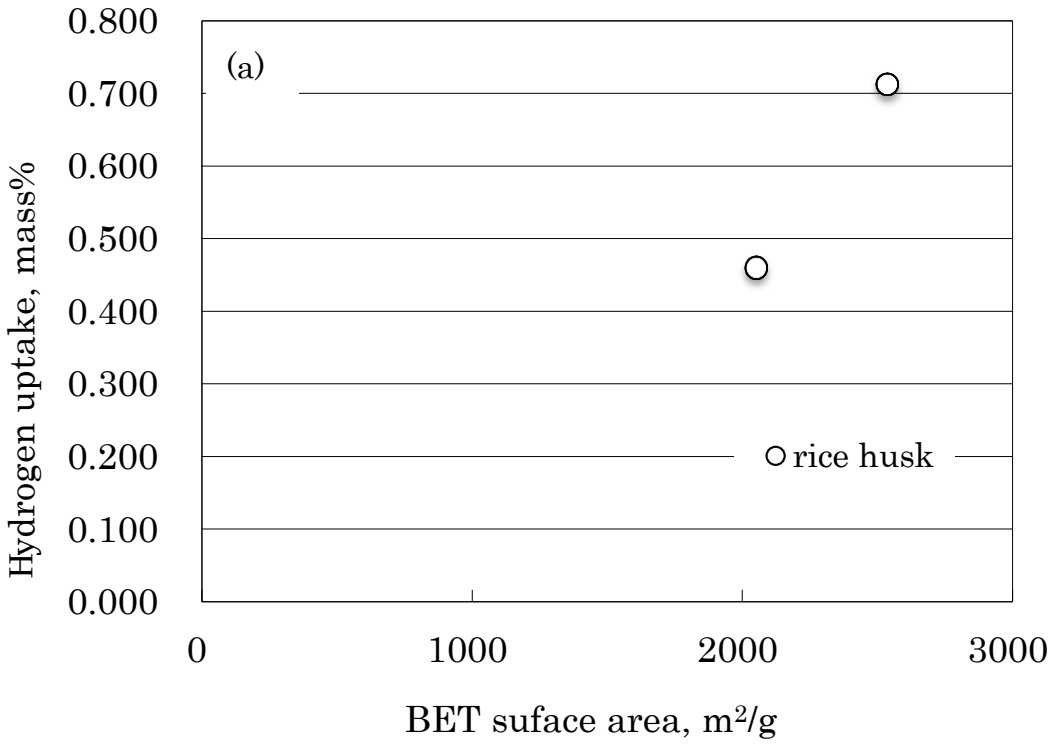

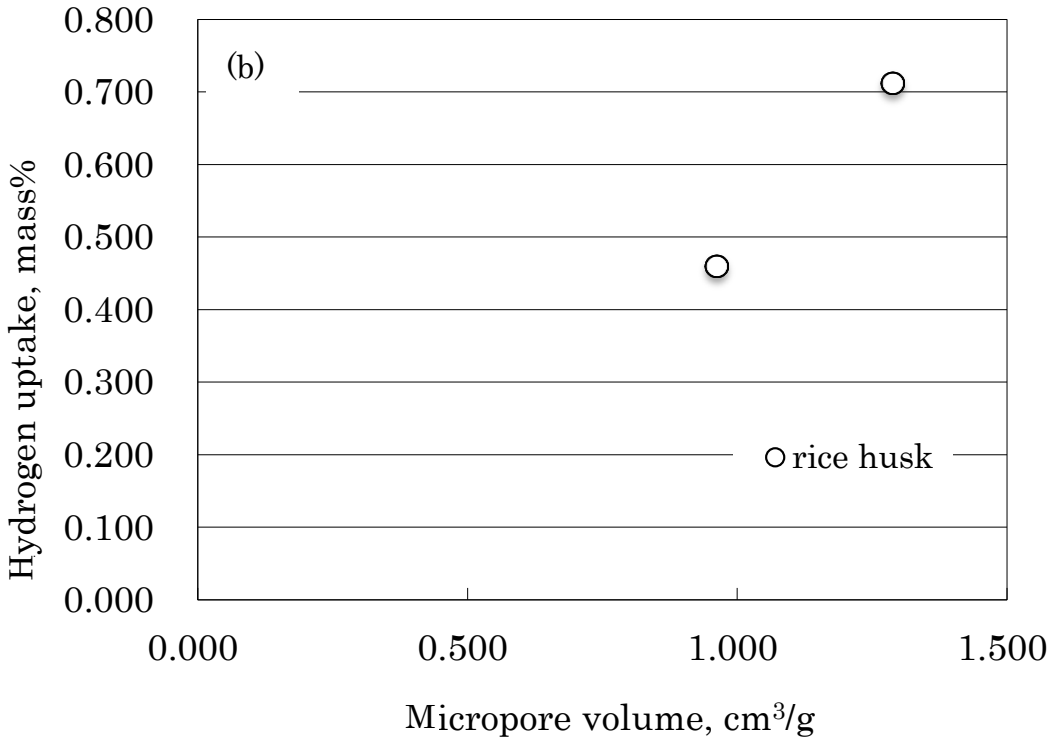

Figure 3.6. Hydrogen uptake vs. micropore volume (at 303 K, 10 MPa).

3.4 Conclusion

Tow KOH activated carbons form rice husk were synthesized. Their porosity characteristics of micropore volume and size, and hydrogen adsorption capacities were measured. With the activated rice husk carbons, higher volumes of micropores and lower volumes of mesopores had formed, as compared to the PAN carbons. The mesopore volume depended on the amount of KOH added. For example, when KOH was added to the raw carbon material at a ratio of four parts to one, a larger number of mesopores formed. The calcination temperature had little effect on the total pore volume, but when calcinated at higher temperatures, the micropore volume decreased. Changing the calcination temperature and amount of KOH had little effect on the pore size distribution. They stored as much as 1.0 mass% of hydrogen at 303 K/27 MPa. These materials could be synthesized with controlled around these micropore sizes by suitable calcination conditions, and showed promise that this could be further improved for actual use.

3.5 Reference

[1] Z. Ryu, H. Rong, J. Zheng, M. Wang, B. Zhang, Microstructure and chemical analysis of PAN-based activated carbon fibers prepared by different activation methods, *Carbon*, **2002**, *40*, 1131–1150.
[2] H. Wang, Q. Gao, and J. Hu, High Hydrogen Storage Capacity of Porous Carbons Prepared by Using Activated Carbon, *J. Am. Chem. Soc*. **2009**, *131*, 7016–7022.
[3] I. Martin-Gullon, J. P. Marco-Lozar, D. Cazorla-Amorós, A. Linares-Solano, Analysis of the microporosity shrinkage upon thermal post-treatment of H_3PO_4 activated carbons, *Carbon*, **2004**, *42*, 1339-1343.
[4] I. Toda, H. Ono, T. Takahata, S. Ohshio, H. Akasaka, S. Himeno, T. Kokubu, H. Saitoh, Hydrogen Storage Property of Nanoporous Carbon Materials Prepared from Rice Husks, *J. Sol. Mech. Mat. Eng.* **2009**, *3*, 1306-1311.

Chapter 4

Structural and Chemical Properties of Lithium Doped Activated Carbons

Abstract

KOH activated carbons made from coke, PAN, rice husk are doped with lithium. KOH activated carbon materials have oxygen-containing functional groups on their surfaces. They can react with the basic lithium reagent. From elemental analysis, it was found that lithium was doped to functional groups in the surface of materials. And the effects of lithium vary depending on the raw materials. Because the lithium reagent can react with the material and alter the pore structure, lithium doping has the effect of plugging or filling the micropores and changing the structures of functional groups, resulting in the formation of mesopores.

4.1 Introduction

I attempted to synthesize activated carbon hydrogen storage materials by KOH activation not only from cokes but for rice husk and PAN fibers because they were expected to show high BET surface areas of around 3000 m^2/g [1]. I designed several sets of activation conditions and investigated porosity by way of adsorption measurements. Then, each material's hydrogen storage capacity was measured at 303 K [2].

To create hydrogen storage materials with better storage capacity, lithium has been introduced onto the surface of porous carbon materials. These lithium-doped hydrogen storage materials have been reported to show increased hydrogen storage capacity. Previous studies have suggested that introducing lithium into a hydrogen storage material enhances the interaction between the hydrogen molecules and the material (Figure 4.1, 4.2)[3-6]. These studies suggest that the hydrogen uptake capacity will increase.

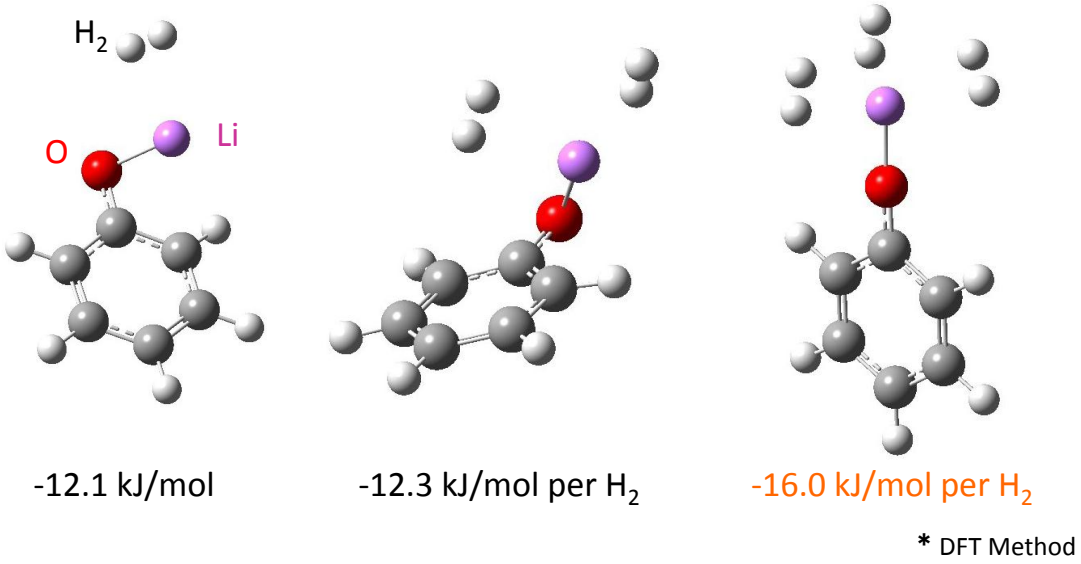

Figure 4.1. DFT calculation results of hydrogen uptake for Lithium doped aromatic structures.

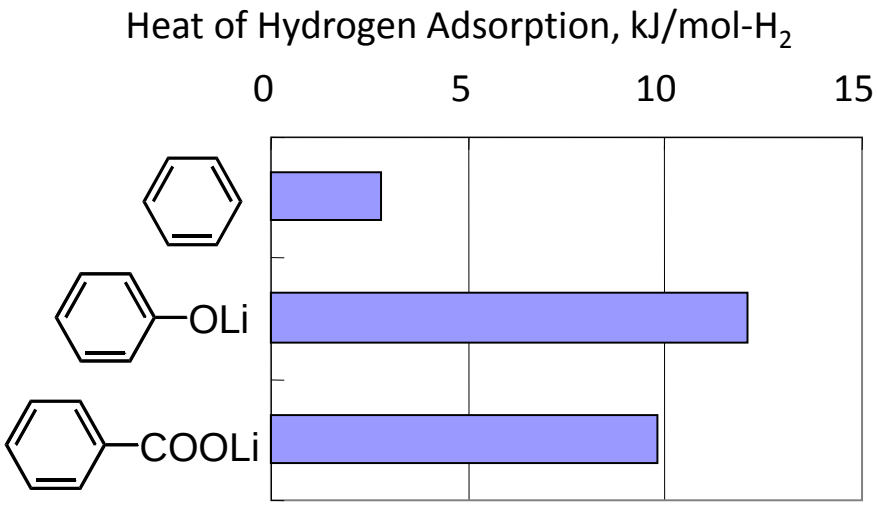

Figure 4.2. The comparison of heat of hydrogen adsorption on to the benzene structure, lithium doped phenol structure and lithium doped benzoic acid structure.

To examine whether the addition of lithium could increase hydrogen storage capacity, lithium-doped carbon materials were synthesized for this study. Because lithium is lightweight, it would be possible to increase hydrogen storage capacity without the drawback of making the material significantly heavier. KOH activated carbon materials have oxygen-containing functional groups on their surfaces (Figure 4.3, 4.4). For example, KOH activated coke carbon have quinone, carboxylic acid, hydroxyl, lactone and carboxylic acid from alkaline titration. These oxygen-containing functional groups are determined by alkaline titration. NaOEt ethanol solution can react with quinone, hydroxyl, lactone and carboxylic acid. NaOH aqueous solution can react with hydroxyl, lactone and carboxylic acid. Na_2CO_3 can react with lactone and carboxylic acid. $NaHCO_3$ can react with carboxylic acid [7]. Because LiOH have comparable basicity of NaOH, LiOH can react with hydroxyl, lactone and carboxylic acid.

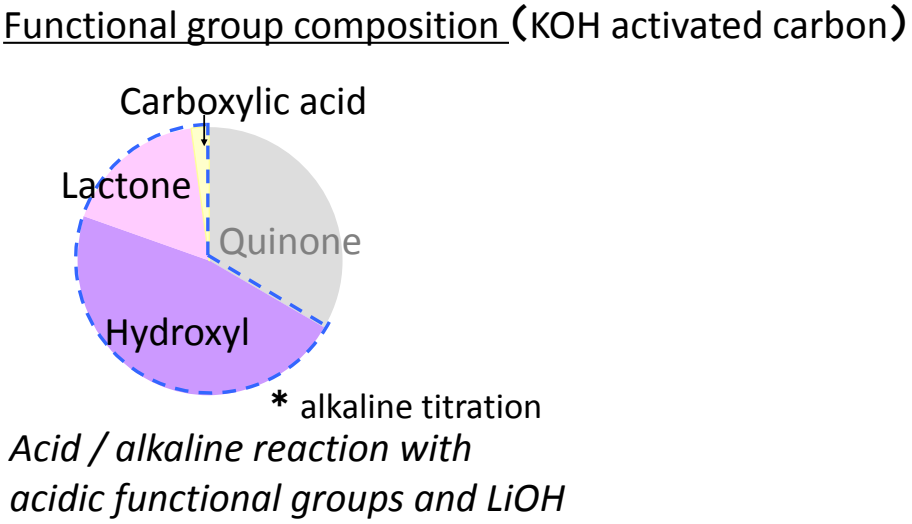

Figure 4.3. The functional group composition of KOH activated cokes carbons measured by alkaline titration (JX Nippon Oil & Energy Corporation).

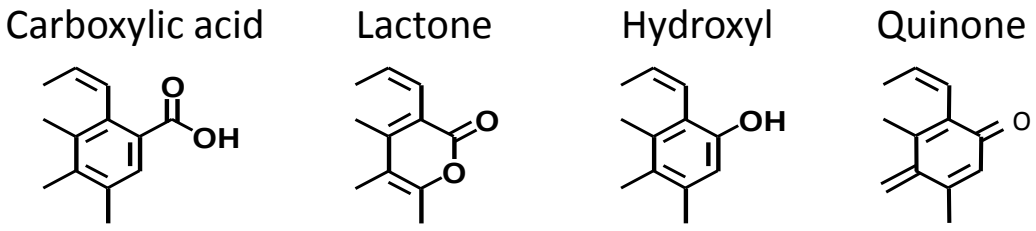

Figure 4.4. The chemical structures of functional groups existing on the surface of KOH activated carbons [7].

LiOH was reacted with the functional groups, which include carboxylic acid and anhydride, in order to introduce lithium into the pore walls in the carbon materials. By reacting lithium with the functional groups present on the inner pore surface, advantage could be taken of the fact that lithium bonds to the material, thereby introducing lithium into the carbon material (Figure 1.4). It is thought that hydrogen storage capacity can be improved without significantly altering the pore structure in the material. The research reported in this paper is aimed at clarifying the effects of lithium doping on porous structures when lithium is introduced for the purpose of increasing hydrogen storage in practical conditions.

4.2 Experimental section

4.2.1 Carbon materials

KOH activated carbons were selected as the initial carbon materials. These included activated cokes carbon (JX Nippon Oil & Energy Corporation), activated PAN carbon and activated rice husk carbon (Environmental Technique Service Co.). The activated PAN carbon is referred as "PAN-B2" in chapter 2. The activated rice husk carbon is referred as "rice husk-1" in chapter 3. The adsorption properties, elemental analysis and alkaline titration analysis results of these KOH activated carbons are listed in Table 4.1. The BET surface area, total pore volume and micropore volume of the activated carbons are shown in Table 4.2.

4.2.2 Lithium doping

Each of the activated carbons selected for lithium doping was vacuum dried at 393 K for 4 hrs. A solution obtained by mixing the dried activated carbon with LiOH (1 molar equivalent of the surface functional groups) and water was then stirred for 4 hours for reaction. Then, the solution was subjected to suction filtration to filter out the solids, and rinsed 5 times with purified water. The rinsed activated carbon was vacuum dried at 373 K for 4 hrs to obtain a lithium-doped activated carbon material (Figure 4.5).

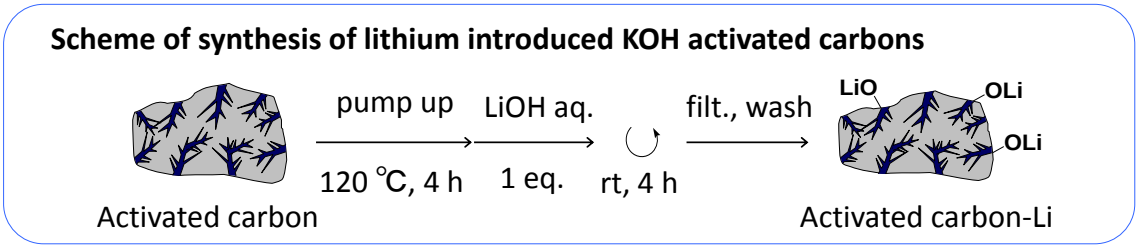

Figure 4.5. Synthesis of lithium doped KOH activated carbons.

4.2.3 Characterization

Transmission electron microscopy images were obtained using a Topcon (EM-002B) microscope operating at 120 kV (measured by Dr. Noriko Yoshizawa of AIST). The BET surface area and pore volume were estimated by nitrogen adsorption measurement at 77 K using a BELsorp-max instrument. Before the nitrogen adsorption measurement, the samples were dried under vacuum at 523 K for 4 hrs.

Elemental analysis was conducted. The analyzer used to estimate the lithium concentration was an ICPS-8100 by Shimadzu Corp. The sample was added to 95% sulfuric acid and heated until carbonized. Then the carbonized sample was heated until became ashed by furnace at 798 K. After that, the ashed sample was added to 35% hydrochloric acid under 423 K. The solution was diluted to 20 times of the volume. The lithium content is shown in Table 4.1.

Table 4.1. Functional groups and lithium content of activated carbons and lithium doped activated carbons.

Sample	Functional groups[a], mmol/g	Li[b], mass%	Li[b], mmol/g
coke	1.2	0	0
coke-Li		0.37	0.53
PAN	0.80	0	0
PAN-Li		0.13	0.19
rice husk	2.2	0	0
rice husk-Li		0.73	1.1

[a] Functional group content was determined by dispersing the material in a 0.05 mol/l NaOH aqueous solution and reacting for 20 hrs, then titrating the remaining bases with a 0.05 mol/l HCl aqueous solution. [b] Lithium content of the activated carbons was determined by ICP emission analysis.

Table 4.2. Properties of activated carbons and lithium doped activated carbons.

Sample	S_{BET}[a], m^2/g	V_t[b], cm^3/g	V_{micro}[c], cm^3/g	V_{meso}[d], cm^3/g	d_P[e], nm
coke	2073	0.98	0.98	0.0	0.8
coke-Li	1890	0.89	0.86	0.03	0.8
PAN	2778	1.84	1.30	0.54	1.3
PAN-Li	2541	1.70	1.23	0.47	1.4
rice husk	2537	1.31	1.29	0.02	0.9
rice husk-Li	2491	1.28	1.18	0.10	0.9

[a] Surface area (S_{BET}) was estimated by the Brunauer-Emmet-Teller (BET) method at a relative pressure of around 0-0.25. [b] V_t shows the total pore volume. [c] Micropore volume (V_{micro}) was calculated by the Dubinin-Radushkevich (DR) method. [d] Mesopore volume was calculated by subtracting the micropore volume from the total pore volume. [e] Peak pore size (d_P) was estimated by the MP method.

4.3 Results and discussion

4.3.1 Lithium elemental analysis

Table 4.1 shows the lithium elemental analysis results of the lithium-doped activated coke carbon, PAN carbon and rice husk carbon treated with LiOH aqueous solution. As the table shows, lithium had bonded to roughly half the functional groups that were initially present in the activated carbon. 0.53 mmol/g of lithium had been introduced into the activated coke, which had 1.2 mmol/g of functional groups. Hence, 44% of the functional groups had reacted with the LiOH. Likewise, the activated PAN carbon originally had 0.80 mmol/g of functional groups and 0.19 mmol/g of lithium was introduced, meaning that 24% of the functional groups had reacted. The activated rice husk carbon had 2.2 mmol/g of functional groups and 1.1 mmol/g of lithium was introduced, meaning that 50% of the functional groups had reacted.

4.3.2 Structural characterization

TEM images are shown in Figure 4.6. They show that the KOH activated carbons consist of stacked graphene layers. These layers have an irregular stacking structure, with defects and edges. These defects usually occur because carbon atoms are missing or because five-membered rings form instead of six-membered rings. The defects result in curving of the graphene layers and formation of walls and pores. The pores appear as white dots in the TEM images, and were observed to be under 2 nm in diameter. The structures vary depending on the raw material of the activated carbon. The KOH activated carbons from PAN were made up of thicker layers than the other carbons, such that the pore size distribution was comparatively uneven.

In comparing the activated carbons before and after lithium doping, it was found that lithium doping had caused structural changes. The fundamental layer structure was maintained but larger pores had formed. These pores were 10 nm in diameter, which puts them in the mesopore range, but this size is not favorable for hydrogen storage [8]. The formation of mesopores was especially pronounced in the activated rice husk carbon.

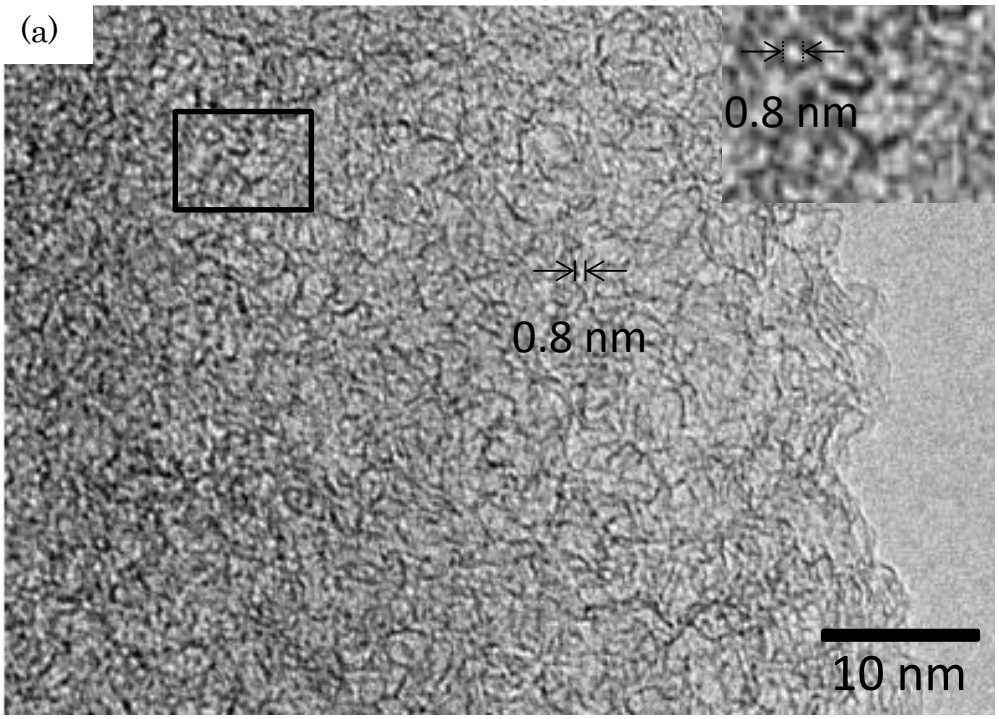
(a)
0.8 nm
0.8 nm
10 nm

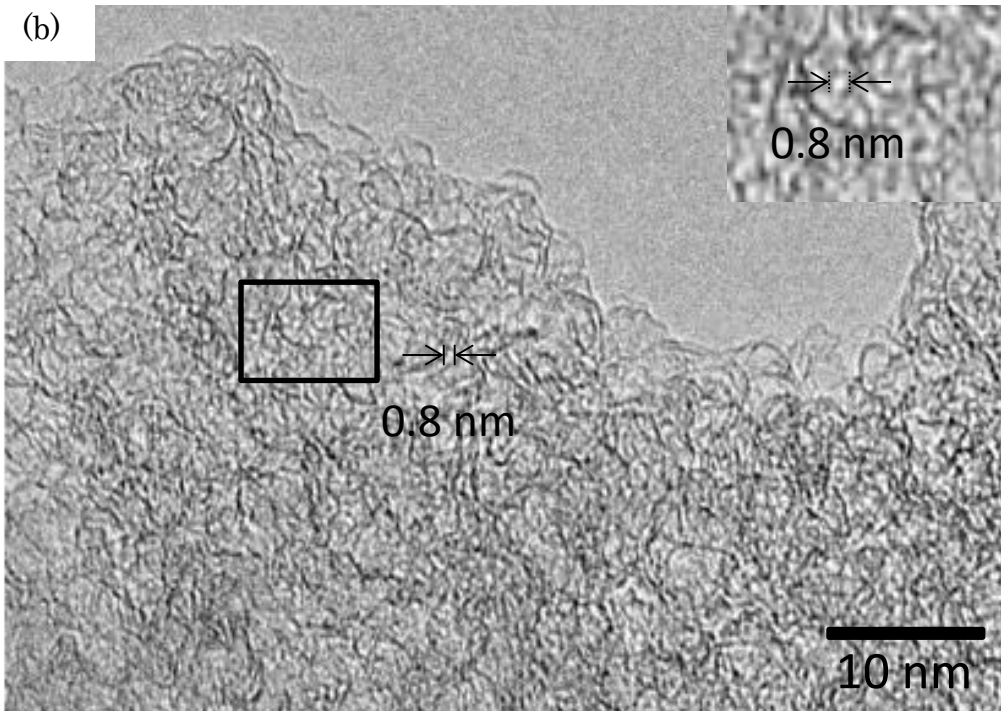
(b)
0.8 nm
0.8 nm
10 nm

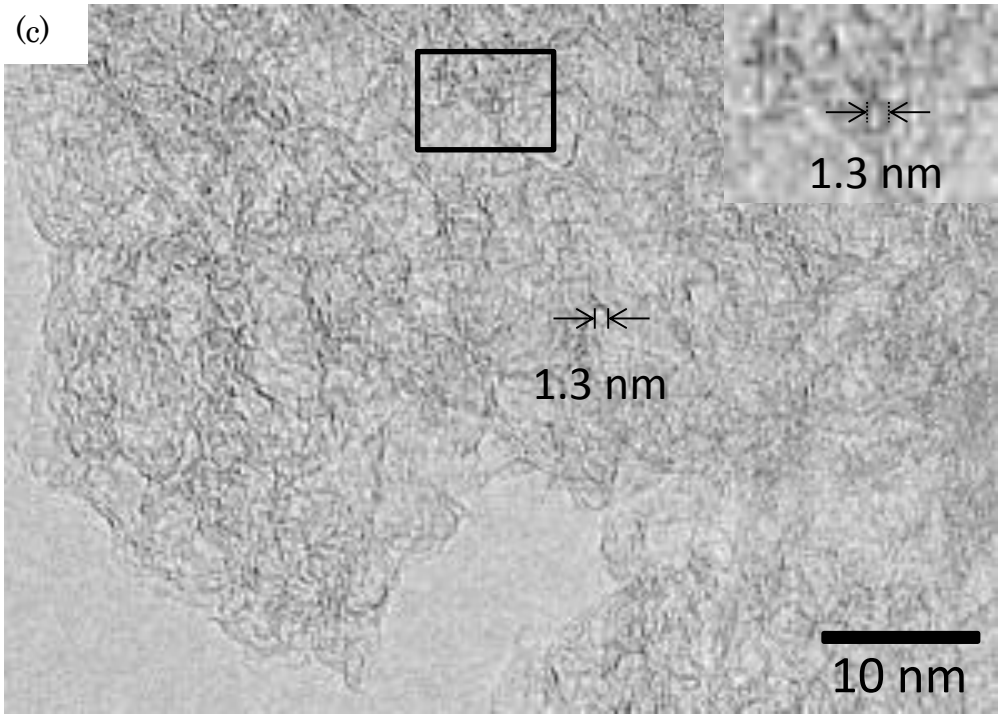
(c)
1.3 nm
1.3 nm
10 nm

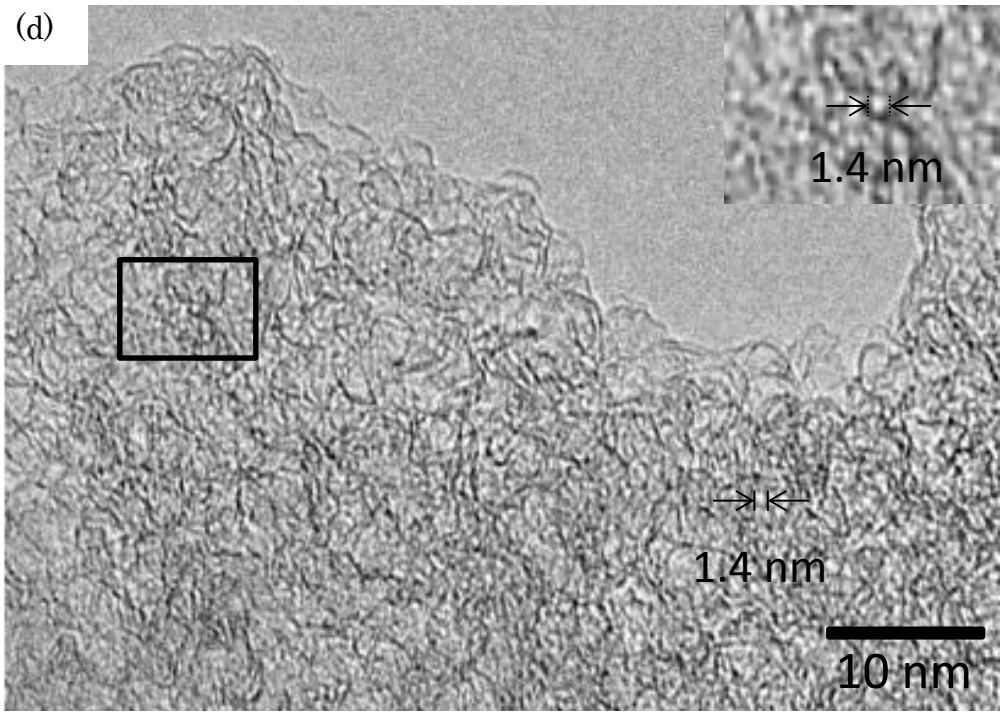
(d)
1.4 nm
1.4 nm
10 nm

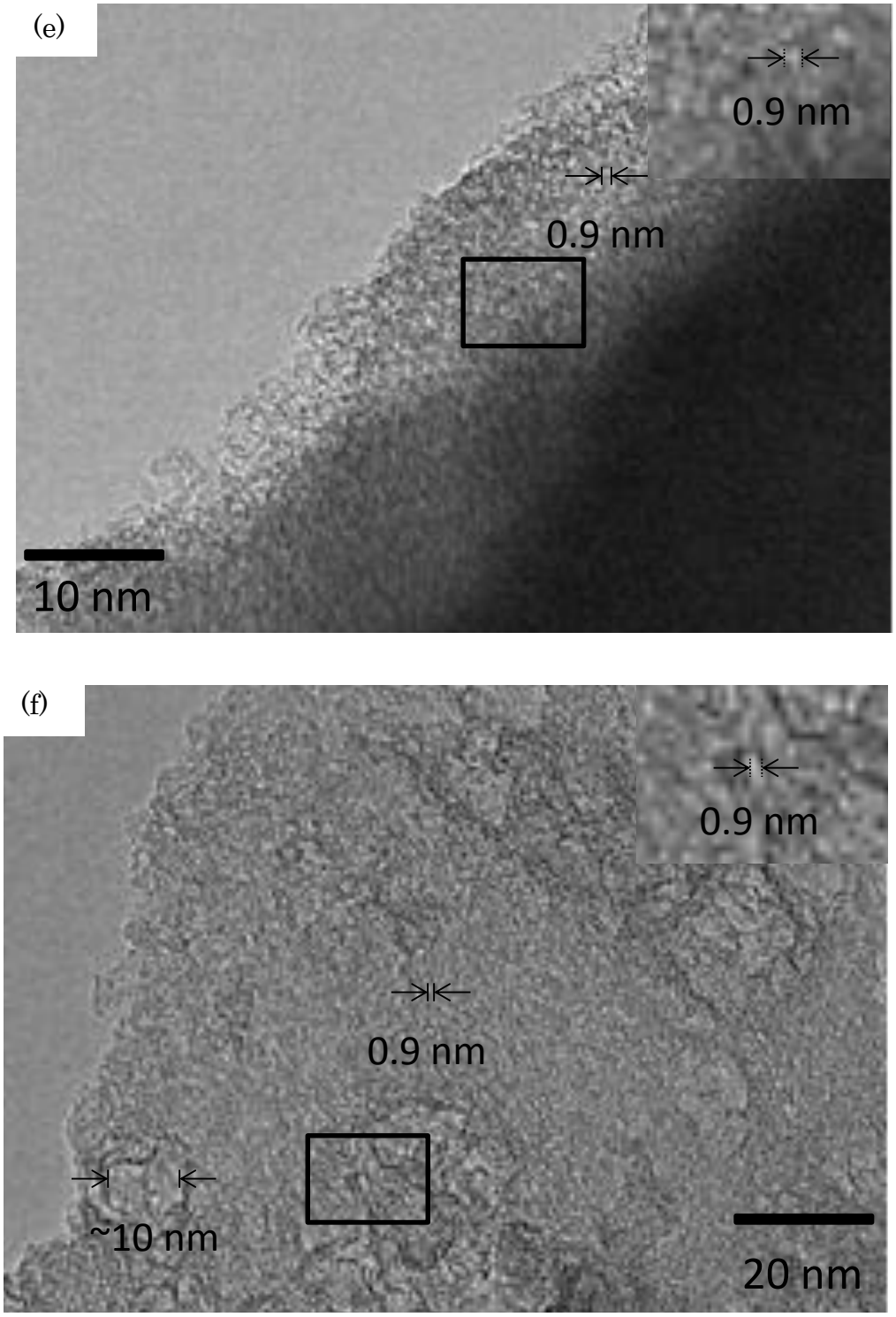

Figure 4.6. TEM images of activated coke carbon (a), activated coke carbon-Li (b), activated PAN carbon (c), activated PAN carbon-Li (d), activated rice husk carbon (e), and activated rice husk carbon-Li (f).

4.3.3 Pore volume estimation

The nitrogen adsorption-desorption isotherms for the KOH activated carbons from coke carbon, PAN carbon and rice husk carbon are shown in Figure 4.7. The figure shows the isotherms for each activated carbon material before and after lithium doping. These isotherms show that adsorption took place at relatively low pressure, which indicates the presence of well developed micropores in the activated carbons.

Looking closely at the isotherms, it was found that the activated coke shows a typical Type-I isotherm. Type-I isotherm is a long horizontal plateau, which extends up to relatively high P/P_0. After lithium introduction, BET surface area decreased significantly, by 9% compared to the initial value, indicating that lithium doping has the effect of plugging or filling the micropores.

In the cases of the activated PAN carbon and rice husk carbon, nitrogen adsorption was also observed in the range of 0.4-0.9, which indicates that small mesopores exist in the structure. These isotherms are of a mixed Type-I and IV [9]. Type-IV occurs on porous adsorbents with pores in the range of 1.5-100 nm. At higher pressures the slope shows increased uptake of adsorbate as pores become filled, inflection point typically occurs near completion of the first monolayer.

The activated PAN carbon showed similar behavior before and after lithium was introduced, and absorbed as much nitrogen as it had initially. But the activated rice husk carbon showed a 2% decrease in nitrogen adsorption compared to the initial value. The isotherm clearly indicates that there are fewer micropores and small mesopores in the lithium-doped rice husk carbon than in the initial activated carbon.

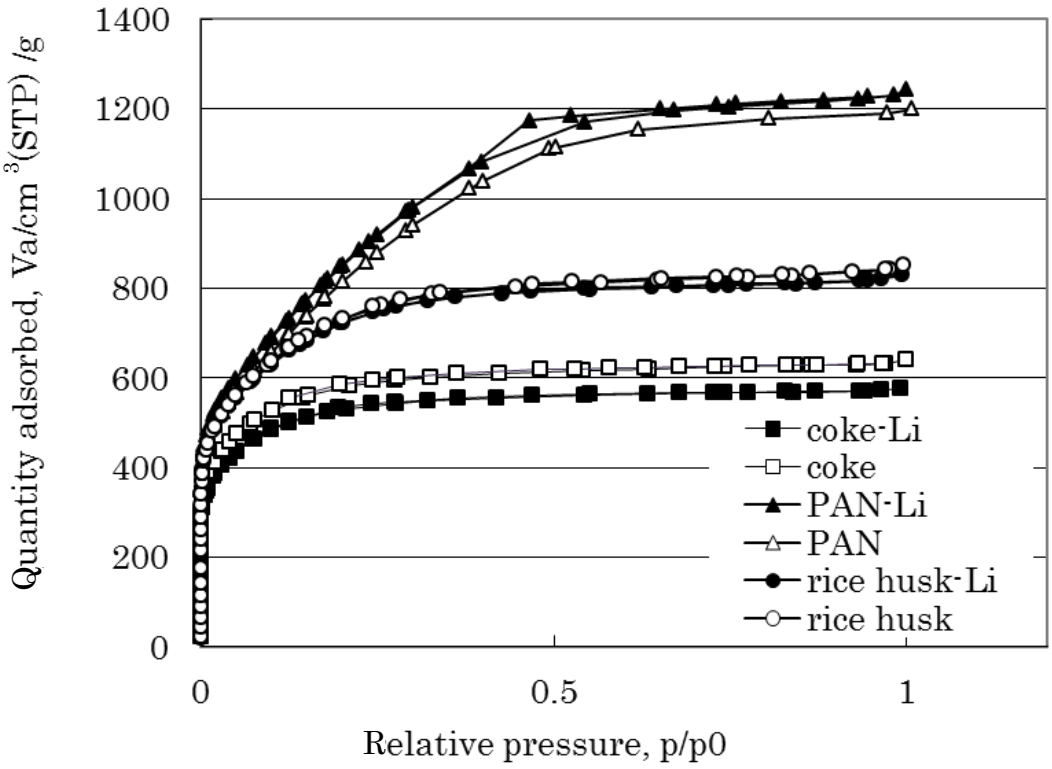

Figure 4.7. Nitrogen adsorption-desorption isotherms of the activated carbons and lithium-doped activated carbons.

Pore size analysis of the lithium-doped activated carbons conducted by the MP method (Figure 4.8-4.11, Figure 2.4 for activated PAN carbon, Figure 3.3 for activated rice husk carbon) showed a pore size distribution of around 0.8 nm for the activated coke carbon, 0.9-1.4 nm for the activated PAN carbon, and 0.9-1.2 nm for the activated rice husk carbon. These smaller pores are more susceptible to being plugged or filled, such that lithium doping caused a slight decline in nitrogen uptake.

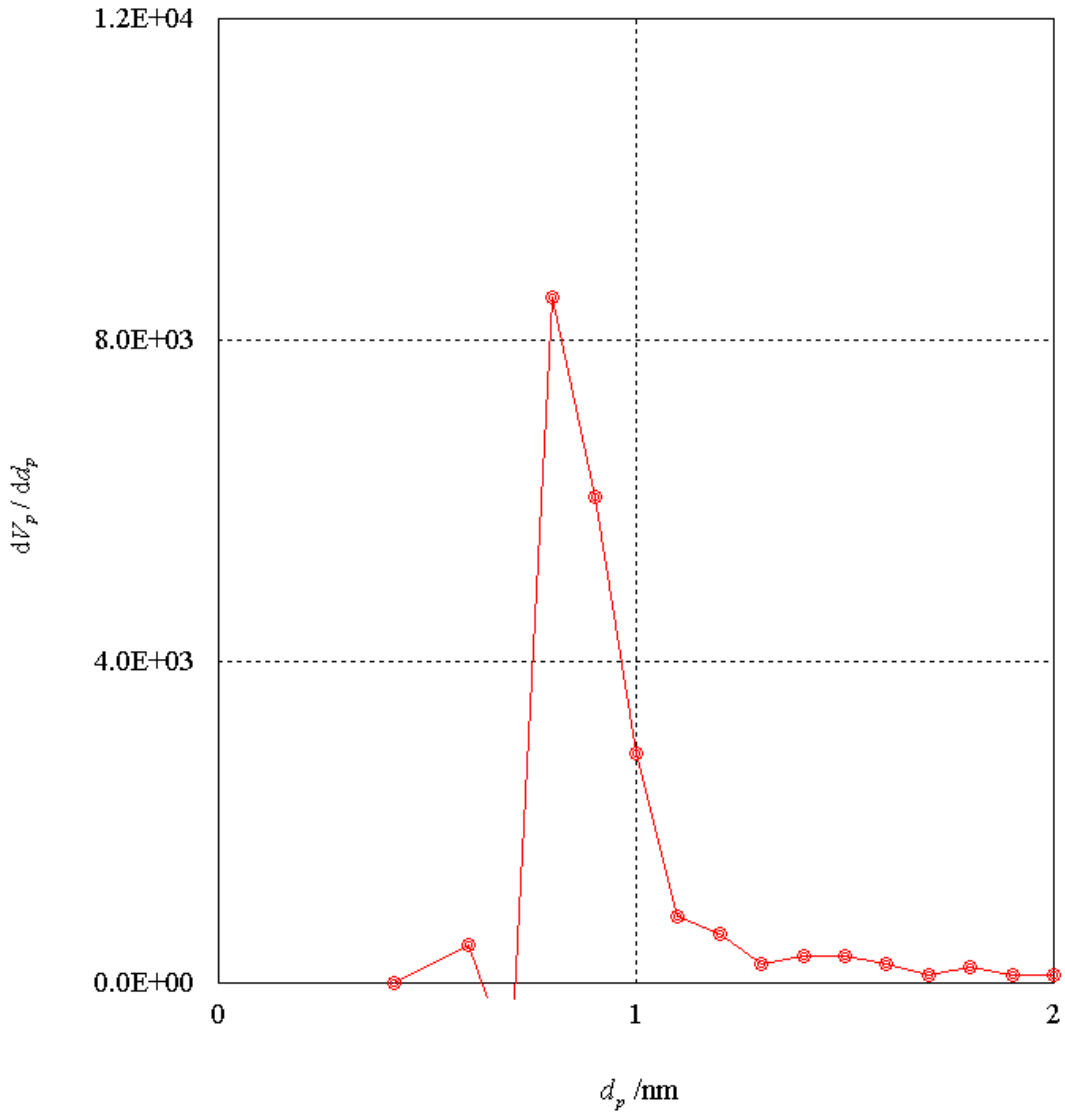

Figure 4.8. MP-plot of KOH activated carbon from coke.

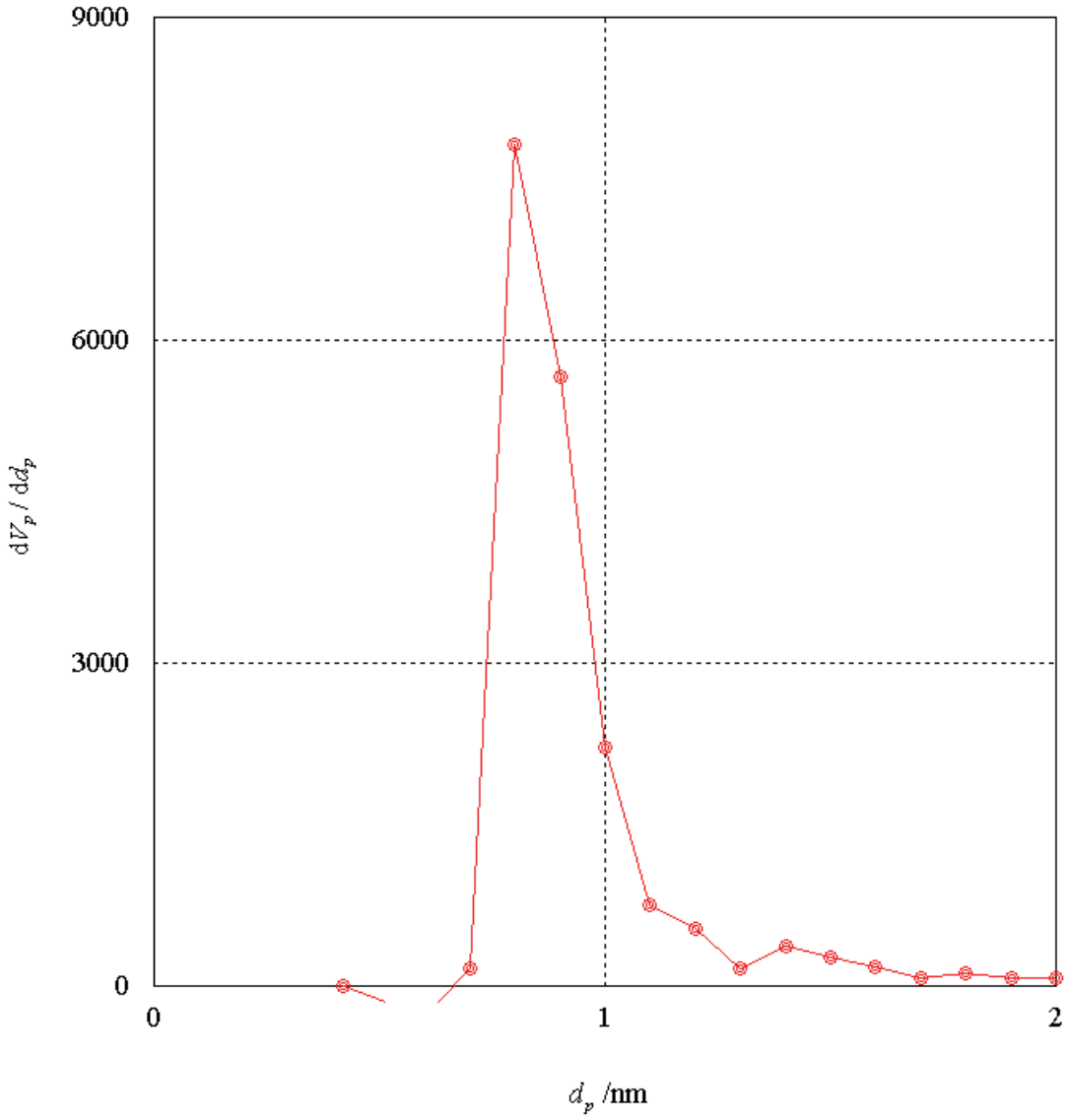

Figure 4.9. MP-plot of lithium-doped KOH activated carbon from coke.

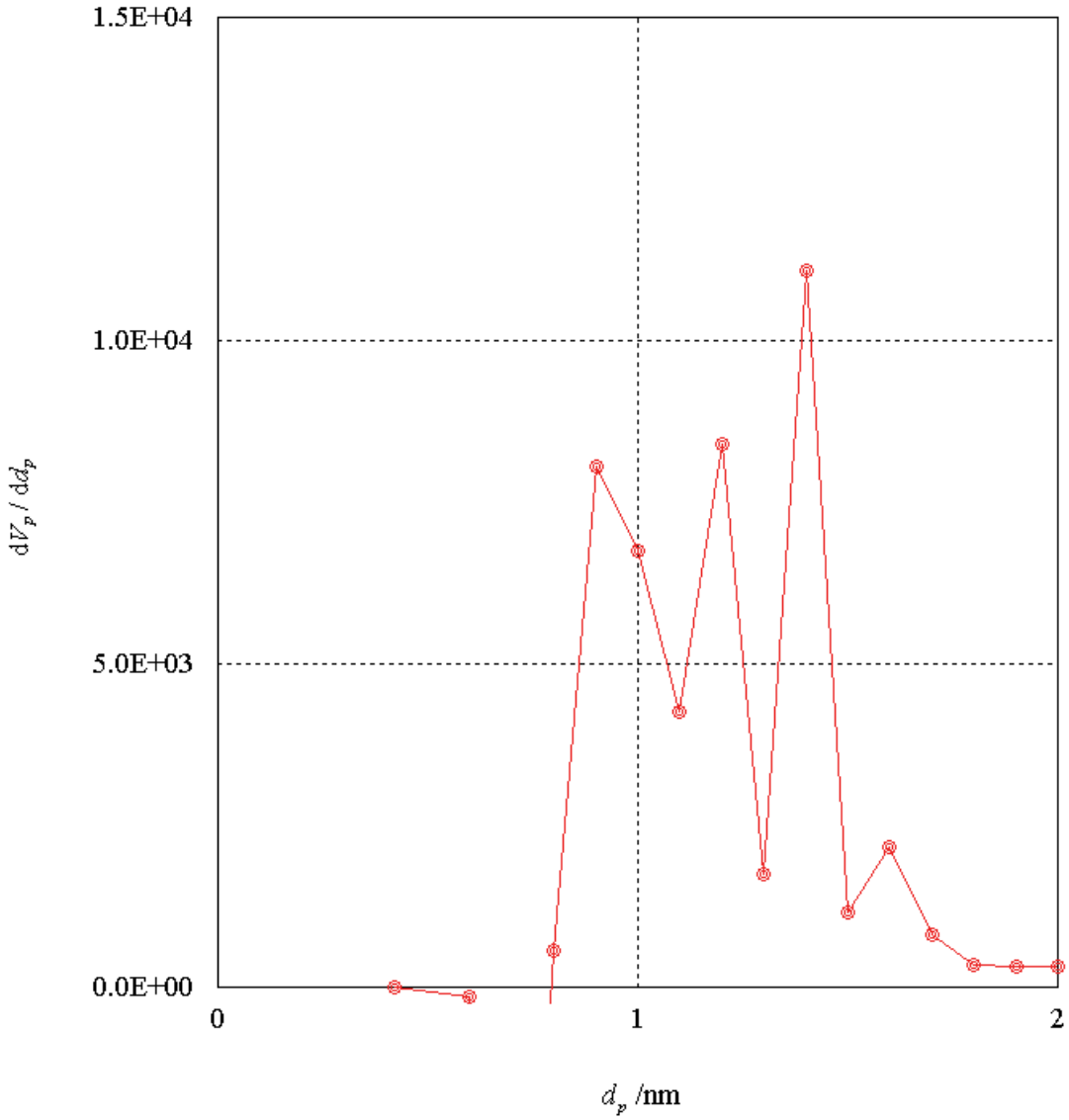

Figure 4.10. MP-plot of lithium-doped KOH activated carbon from PAN.

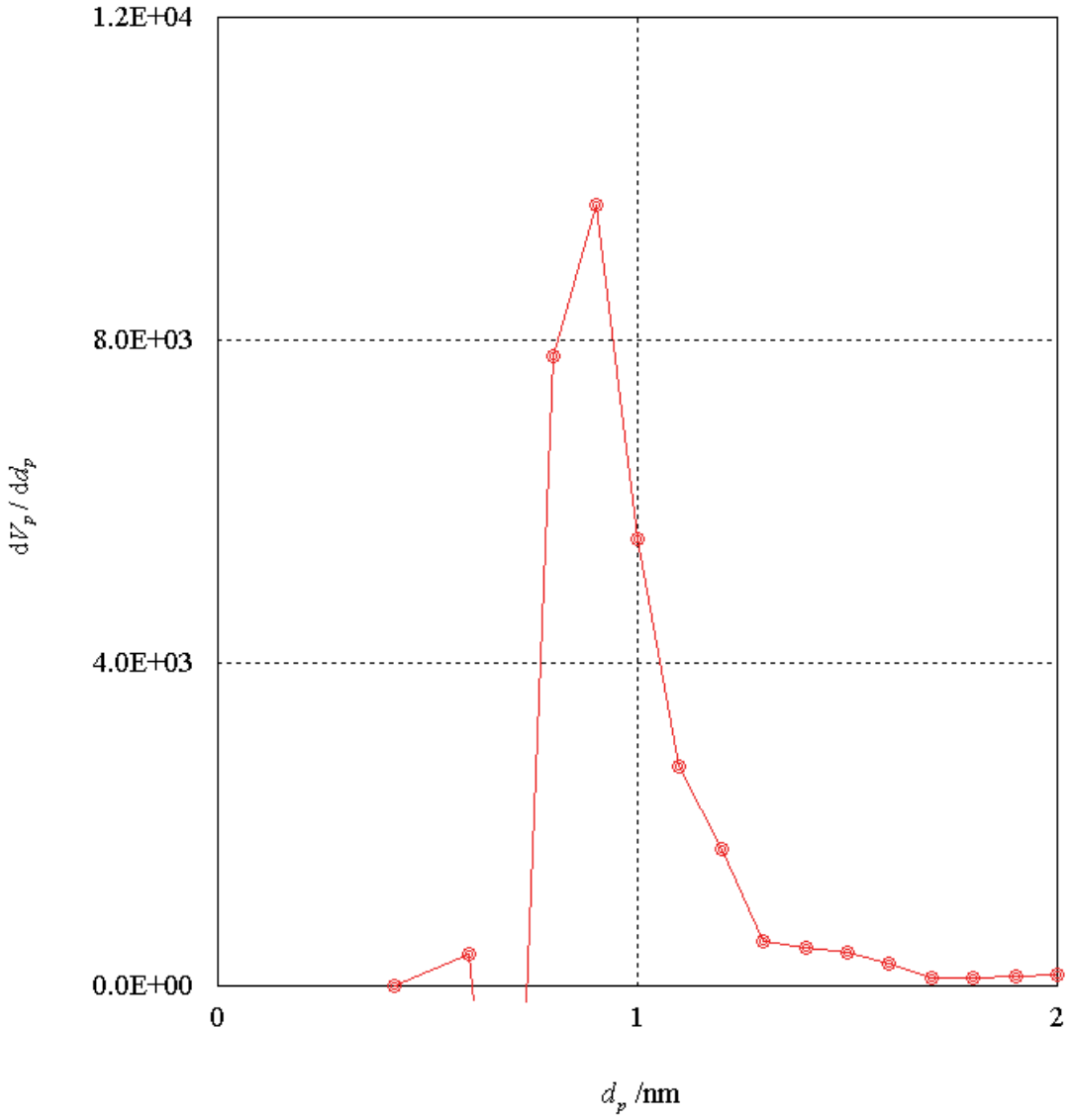

Figure 4.11. MP-plot of lithium-doped KOH activated carbon from rice husk.

4.3.4 Functional groups characterization

To study the pores observed in the lithium-doped activated rice husk (shown in TEM image in Figure 4.6(f)), the functional groups were characterized. The temperature programmed desorption method (TPD) was used to study changes in the functional groups (measured by Dr. Hideyuki Takagi of AIST). The TPD measurement results are shown in Figure 4.12. After lithium doping, the decrease in CO desorption around 800 K indicates that the anhydride structure had been decomposed, while the decrease in CO_2 desorption around 1100 K indicates that the ether, quinone and carbonyl structures had been decomposed. The increase in CO_2 desorption around 500 K and increase in CO desorption around 1000 K indicate that carboxyl and phenol structures had formed through the reaction with the LiOH aqueous solution [10].

Table 4.3. Estimated functional group content of activated rice husk and activated rice husk-Li as determined by Temperature Programmed Desorption (TPD).

Sample	Desorbed species	Amount of functional groups, mmol/g	
rice husk	CO	1.982	2.339
	CO_2	0.357	
rice husk-Li	CO	1.755	2.564
	CO_2	0.809	

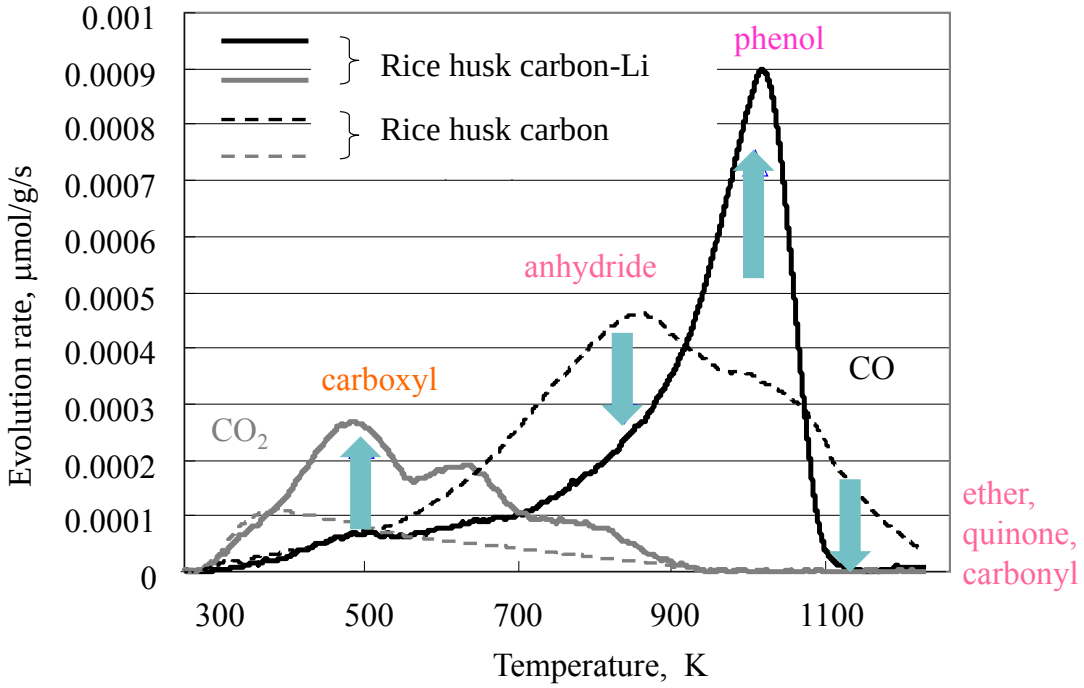

Figure 4.12. Temperature programmed desorption (TPD) of activated rice husk carbon (dashed line), and activated rice husk carbon-Li (solid line).

These results indicate that reaction with LiOH causes changes in the functional groups due to hydrolytic cleavage of the existing covalent bonds. Through hydrolytic cleavage, ether groups become hydroxyl groups, and anhydride groups become carboxyl groups (Figure 4.13). Thus, it is possible that bond cleavage caused the pore sizes to become larger, as seen in Figure 4.6(f), and the micropore volume to decrease.

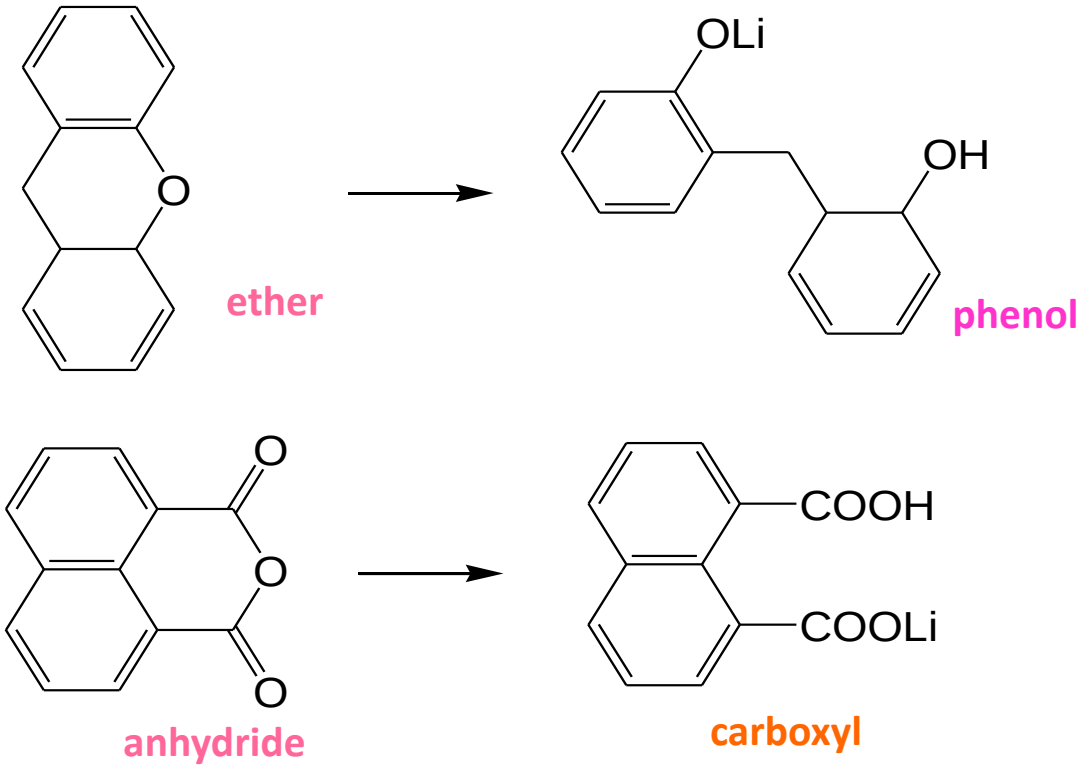

Figure 4.13. Chemical structure changing of functional groups by hydrolytic cleavage with LiOH aqueous solution.

4.4 Conclusion

I succeeded in introducing lithium into the surface of activated carbons. Lithium was introduced by reacting LiOH with functional groups found on the surface of the activated carbons. The BET surface area of the original activated coke was 2073 m^2/g, while that of the activated PAN carbon and activated rice husk carbon was 2778 m^2/g and 2537 m^2/g, respectively. After being treated with the LiOH aqueous solution, the activated coke showed a decrease in BET surface area of 8%, while the hydrogen storage capacity was nearly the same as before lithium doping. The effects of lithium vary depending on the characteristics of the initial activated carbon. Nitrogen adsorption measurements show that lithium doping causes a decrease in the number of micropores and, as the TEM images show, results in formation of relatively large pores.

4.5 Reference

[1] Z. Ryu, H. Rong, J. Zhen, M. Wang, B. Zhang. Microstructure and chemical analysis of PAN-based activated carbon fibers prepared by different activation methods. *Carbon*, **2002**, *40*, 1131–1150.
[2] A. Minoda, S. Oshima, H. Iki, E. Akiba. Synthesis of KOH-activated porous carbon materials and study of hydrogen adsorption, *Journal of Alloys and Compounds*, **2013**, *580*, S301-S304.
[3] S. S. Han, W. A. Goddard. Lithium-Doped Metal-Organic Frameworks for Reversible H_2 Storage at Ambient Temperature, *J. Am. Chem. Soc*. 2007, *129*, 8422-8423.
[4] H. Tachikawa, A. Shimizu. Diffusion Dynamics of the Li^+ Ion on a Model Surface of Amorphous Carbon: A Direct Molecular Orbital Dynamics Study. *J. Phys. Chem. B* **2005**, *109*, 13255-13262.
[5] A. Mavrandonakis, E. Tylianakis, A. K. Stubos, G. E. Froudakis. Why Li Doping in MOFs Enhances H_2 Storage Capacity? A Multi-scale Theoretical Study. *J. Phys. Chem. C* **2008**, *112*, 7290-7294.
[6] W. Liu, Y. H. Zhao, Y. Li, Q. Jiang, E. J. Lavernia. Enhanced Hydrogen Storage on Li-Dispersed Carb. *J. Phys. Chem. C* **2009**, *113*, 2028–2033.
[7] R. C. Bansal, J. B. Donnet, F. Stoeckli, *Active Carbon*, **1988**, Marcel Dekker, INC, New York and Basel.
[8] H. Wang, Q. Gao, and J. Hu, High Hydrogen Storage Capacity of Porous Carbons Prepared by Using Activated Carbon, *J. Am. Chem. Soc.* **2009**, *131*, 7016–7022.
[9] H. Wang, Q. Gao, J. Hu. High Hydrogen Storage Capacity of Porous Carbons Prepared by Using Activated Carbon. *J. Am. Chem. Soc*. **2009**, *131*, 7016–7022.
[10] H. Takagi, Analysis of surface structure of carbon materials by using temperature-programmed desorption method. *Tanso,* **2009**, *237*, 67-71.

Chapter 5

Hydrogen Storage by Lithium Doped Activated Carbons

Abstract

Several types of lithium-doped KOH activated carbons show higher hydrogen storage affinity than before lithium doped. In the case of activated cokes, lithium doping improves their hydrogen adsorption affinity from 5.02 kg/m^3 to 5.86 kg/m^3 at 303 K. Hydrogen adsorption density increases by around 17% after lithium doping, which indicates that lithium doping is more effective for materials with micropores of 0.8 nm or smaller than 0.8. The activated PAN carbon, improved from 4.60 to 4.83 kg/m^3. Lithium improved the hydrogen adsorption affinity of the activated rice husk from 5.12 kg/m^3 to 5.33 kg/m^3. Despite an observed decrease in hydrogen uptake, lithium doping was found to improve hydrogen adsorption affinity.

5.1 Introduction

I attempted to synthesize activated carbon for hydrogen storage materials by KOH activation not only from cokes but also rice husk and PAN fibers because they can produce at low-cost and had availability in large volume, and expected to show high BET surface areas of around 3000 m^2/g [1]. I designed several sets of activation conditions and investigated porosity by way of adsorption measurements. Then, each material's hydrogen storage capacity was measured at 303 K [2].

To create hydrogen storage materials with better storage capacity, lithium has been introduced onto the surface of porous carbon materials. These lithium-doped hydrogen storage materials have been reported to show increased hydrogen storage capacity [3]. Previous studies have suggested that introducing lithium into a hydrogen storage material enhances the interaction between the hydrogen molecules and the material [3-6]. These studies suggest that the hydrogen uptake capacity will increase. To examine whether the addition of lithium can increase hydrogen storage capacity, lithium-doped carbon materials were synthesized for this study. Because lithium is lightweight, it is possible to increase hydrogen storage capacity without the drawback of making the material significantly heavier. KOH activated carbon materials have oxygen-containing functional groups on their surfaces. LiOH was reacted with the functional groups, which include carboxylic acid and anhydride, in order to introduce lithium into the pore walls in the carbon materials. By reacting lithium with the functional groups present on the inner pore surface. The advantage could be taken of the fact that lithium bonds to the material, thereby introducing lithium into the carbon material. It is thought that hydrogen storage capacity can be improved without significantly altering the pore structure in the material because lithium atom has under 0.1 nm ionic diameter. The research reported in this paper is aimed at clarifying the effects of lithium doping on porous structures when lithium is introduced for the purpose of increasing hydrogen storage capacity under practical conditions.

5.2 Experimental section

5.2.1 Lithium doped carbon materials

KOH activated carbons were selected as the initial carbon materials. These included activated cokes carbon (JX Nippon Oil & Energy Corporation), activated PAN carbon and activated rice husk carbon (Environmental Technique Service Co.). The activated PAN carbon is referred as "PAN-B2" in chapter 2. The activated rice husk carbon is referred as "rice husk-1" in chapter 3.

Each of the activated carbons selected for lithium doping was vacuum dried at 393 K for 4 hrs. A solution obtained by mixing the dried activated carbon with LiOH (1 molar equivalent of the surface functional groups) and water was then stirred for 4 hours for reaction. Then, the solution was subjected to suction filtration to filter out the solids, and rinsed 5 times with purified water. The rinsed activated carbon was vacuum dried at 373 K for 4 hrs to obtain a lithium-doped activated carbon material (described in chapter 4). The BET surface area, total pore volume and micropore volume of the activated carbons are shown in Table 5.1.

5.2.2 Hydrogen adsorption measurements

Hydrogen adsorption was measured by the volumetric method (hydrogen storage capacity measuring apparatus by Fuse Technonet Co., LTD). Before the measurement, the samples were dried under vacuum at 523 K for 4 hrs. In the pressure vessel the sample was degassed and was maintained at 303 K. After closing the valve connected to the pressure vessel, the pressure in the hydrogen reservoir was controlled for introducing hydrogen. After closing the pressure vessel, the equilibrium pressure was obtained in the hydrogen reservoir and sample cell. The stored hydrogen content in the sample was calculated from the pressure drop measured by pressure gauge. The stored contents were expressed as weight ration of hydrogen (mass%) on total weight. Measurements were performed under various pressures: 0-12 MPa or 0-35 MPa at 303 K, and 0-1 MPa at 77 K.

5.3 Results and discussion

5.3.1 Hydrogen adsorption

The hydrogen storage capacity of the activated carbons mentioned above was measured up to 12 MPa at 303 K, using the volumetric method. Figure. 5.1 shows the hydrogen adsorption isotherms of the activated coke carbon, PAN carbon and rice husk carbon before and after lithium doping. With their larger pore volumes, the activated PAN carbon and rice husk carbon showed greater hydrogen storage capacity than the activated coke carbon. In the case of the activated coke carbon and activated PAN carbon, hydrogen uptake was almost the same after lithium doping as it was initially at 8.8 MPa. On the other hand, the amount of hydrogen adsorbed by the lithium-doped activated rice husk carbon decreased slightly to 5% at 8.8 MPa.

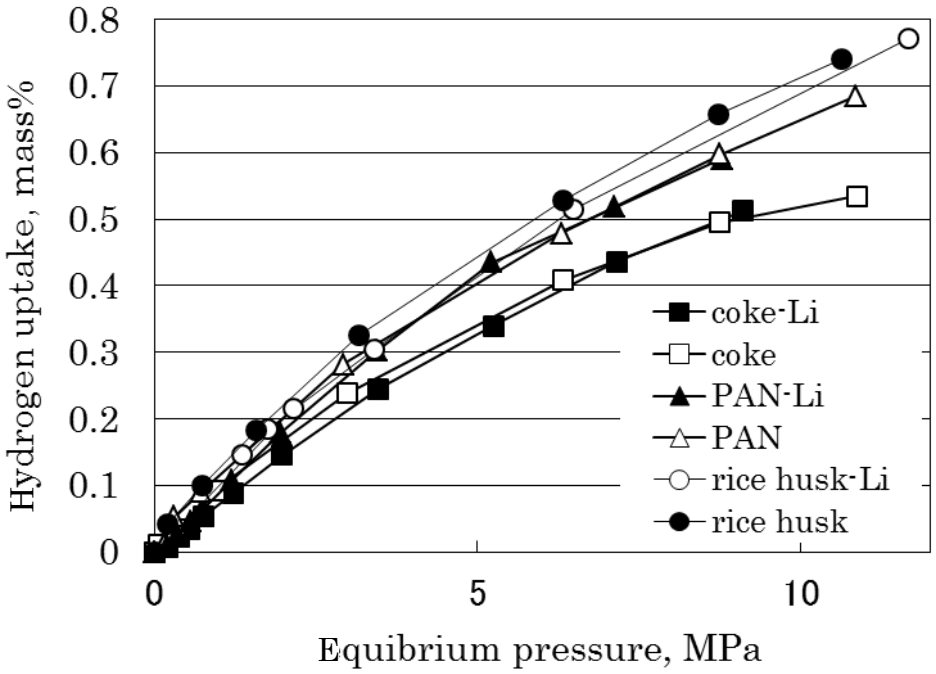

Figure 5.1. Hydrogen adsorption isotherms of the activated carbons and lithium-doped activated carbons.

Table 5.1 shows the hydrogen storage capacities of the activated carbons at 303 K and a hydrogen equilibrium pressure of 8.8 MPa. To closely examine the effect of lithium on hydrogen uptake, I calculated hydrogen adsorption per unit of micropore volume and compared these values among the materials. Hydrogen adsorption affinity was calculated by hydrogen uptake divided by micropore volume based on nitrogen adsorption measurements, and indicates the hydrogen storage capacity per unit micropore volume. The hydrogen storage affinity for the activated coke carbon was calculated at about 5.02 kg/m^3, and 5.86 kg/m^3 after lithium doping; that for the activated rice husk carbon was about 5.12 kg/m^3, and 5.33 kg/m^3 after lithium doping. In terms of hydrogen adsorption affinity, it is clear that lithium doping can improve hydrogen adsorption properties, depending on the carbon material. It can be said that when the micropore size is small, as in under 0.8 nm, lithium has a greater positive effect on hydrogen adsorption affinity than other materials with 0.9-1.4 nm.

Table 5.1. Hydrogen storage properties at 303 K of activated carbons and lithium-doped activated carbons

Sample	S_{BET}[a], m^2/g	V_t[b], cm^3/g	V_{micro}[c], cm^3/g	Hydrogen uptake[d], mass%	Hydrogen adsorption affinity[e], kg/m^3
coke	2073	0.98	0.98	0.496	5.02
coke-Li	1890	0.89	0.86	0.501	5.86
PAN	2778	1.84	1.30	0.599	4.60
PAN-Li	2541	1.70	1.23	0.592	4.83
rice husk	2537	1.31	1.29	0.660	5.12
rice husk-Li	2491	1.28	1.18	0.629	5.33

[a] Surface area (S_{BET}) was estimated by the Brunauer-Emmet-Teller (BET) method at a relative pressure around 0-0.25. [b] V_t shows the total pore volume. [c] Micropore volume (V_{micro}) was calculated using the Dubinin-Radushkevich (DR) method. [d] Hydrogen uptake at 303 K, 8.8 MPa. [e] Hydrogen adsorption affinity calculated as hydrogen uptake divided by micropore volume.

5.4 Conclusion

I succeeded in introducing lithium into the surface of activated carbons. Lithium was introduced by reacting LiOH with functional groups found on the surface of the activated carbons. After being treated with the LiOH aqueous solution, by a close study of the effects of lithium doping on hydrogen storage behavior showed that hydrogen adsorption affinity was most improved in the activated coke carbon. Hydrogen affinity increased by around 17% after lithium doping, likely due to the fact that lithium doping is effective for materials with micropores of 0.8 nm or smaller. Lithium doping improved the hydrogen adsorption affinity of the activated coke carbon from 5.02 to 5.86 kg/m^3. Lithium did not greatly affect the porosity of the activated PAN carbon, and also increase the hydrogen adsorption affinity from 4.60 to 4.83 kg/m^3. Lithium improved the hydrogen adsorption affinity of the activated rice husk carbon from 5.12 to 5.33 kg/m^3. The effects of lithium vary depending on the characteristics of the initial activated carbon. But lithium doping improves hydrogen adsorption affinity. It is possible with lithium doping to increase hydrogen storage uptake by optimization of pore size and functional groups composition.

5.5 Reference

[1] Z. Ryu, H. Rong, J. Zhen, M. Wang, B. Zhang. Microstructure and chemical analysis of PAN-based activated carbon fibers prepared by different activation methods. *Carbon*, **2002**, *40*, 1131-1150.
[2] A. Minoda, S. Oshima, H. Iki, E. Akiba. Synthesis of KOH-activated porous carbon materials and study of hydrogen adsorption. *Journal of Alloys and Compounds*, **2013**, *580*, S301-S304.
[3] S. S. Han, W. A. Goddard. Lithium-Doped Metal-Organic Frameworks for Reversible H_2 Storage at Ambient Temperature. *J. Am. Chem. Soc*. 2007, *129*, 8422-8423.
[4] H. Tachikawa, A. Shimizu. Diffusion Dynamics of the Li^+ Ion on a Model Surface of Amorphous Carbon: A Direct Molecular Orbital Dynamics Study. *J. Phys. Chem. B* **2005**, *109*, 13255-13262.
[5] A. Mavrandonakis, E. Tylianakis, A. K. Stubos, G. E. Froudakis. Why Li Doping in MOFs Enhances H_2 Storage Capacity? A Multi-scale Theoretical Study. *J. Phys. Chem. C* **2008**, *112*, 7290-7294.
[6] W. Liu, Y. H. Zhao, Y. Li, Q. Jiang, E. J. Lavernia. Enhanced Hydrogen Storage on Li-Dispersed Carb. *J. Phys. Chem. C* **2009**, *113*, 2028–2033.

Chapter 6

Conclusion

Conclusion

This thesis describes the study of activated porous carbon for application of hydrogen storage materials. In the carbon structure, micropores are produced by the activation. These porous carbon materials adsorb and desorb large amount of hydrogen at ambient temperature. From this reason, the porous carbons are highly expected to be applied for hydrogen storage.

Chapter 1 deals with the background and general description of this study. The applications of porous materials, such as porous carbon materials and metal organic frameworks for hydrogen storage materials are shown. In this study, I aimed to obtain hydrogen storage materials suitable for practical use around ambient temperatures and hydrogen tank pressure. The purpose is to develop a means of transporting hydrogen gas in a compact manner. So, hydrogen storage materials from activated carbon have been studied. Activated carbons are low-cost, good hydrogen gas accessibility at around ambient temperatures. Chapter 2 describes hydrogen storage of KOH activated carbon from PAN(Poly-acrylonitrile). KOH activated carbon made from PAN has 2625-3145 m^2/g BET specific surface areas. And then, the micropore diameter is 0.9-1.5 nm. The hydrogen storage capacity is 1.1 mass% at 303 K, 30 MPa. Chapter 3 describes hydrogen storage of KOH activated carbon made from rice husk. KOH activated carbon made from rice husk has 0.9 nm micropore diameter, relatively high hydrogen storage property than KOH activated carbon from PAN. Chapter 4 describes structural and chemical properties of lithium doped KOH activated carbons. Synthesized porous carbon materials showed in chapter 2 and 3 and KOH activated carbons from coke are doped with lithium. From elemental analysis, lithium was doped in functional groups. And it showed the lithium doping effect for porous structures varies depending on materials. Chapter 5 describes the hydrogen storage capacity of lithium doped KOH activated carbon materials. Hydrogen adsorption affinity of the activated coke improved from 5.02 kg/m^3 to 5.86 kg/m^3 by lithium doping. The activated carbon from PAN, improved from 4.60 to 4.83 kg/m^3. Lithium improved the hydrogen adsorption affinity of the activated carbon from rice husk from 5.12 kg/m^3 to 5.33 kg/m^3.

From those results of hydrogen storage capacity of lithium doped activated carbons in this thesis, the hydrogen uptake cannot be reach enough such as 5

mass% to use commercially, but I consider that it is possible that lithium doping increase hydrogen uptake by optimization of pore size and functional groups composition. Micropores of sizes smaller than 0.8 nm are preferable, so that it will be effective such smaller micropores are made uniformely. But as in the case of KOH activated carbon from coke, just an optimizing micropore size will cause micropore volume decreasing. It is thought to be the functional group is distributed to around surface of the pore non-uniformly or micropore gate. So, for example, the functional groups distribution on the surface of the pore is examined and uniform lithium introduction will be applicable. Not only lithium but other light metals doping will be the good for hydrogen affinity. And also, it is considerable that carbon materials functionalized with main structure. By doping lithium to functional group on the surface, in all three types of the activated carbon hydrogen storage affinity increased. In order to avoid decreasing micropore volume, the main structure of carbon could be functionalized. Graphene like carbon sheets with framework doped by heteroatom will make one candidate to examine the effect for hydrogen storage capacities. Finally, I expect that metal doped carbon materials realize hydrogen storage and transportation in a compact manner and contribute to establish the hydrogen society.

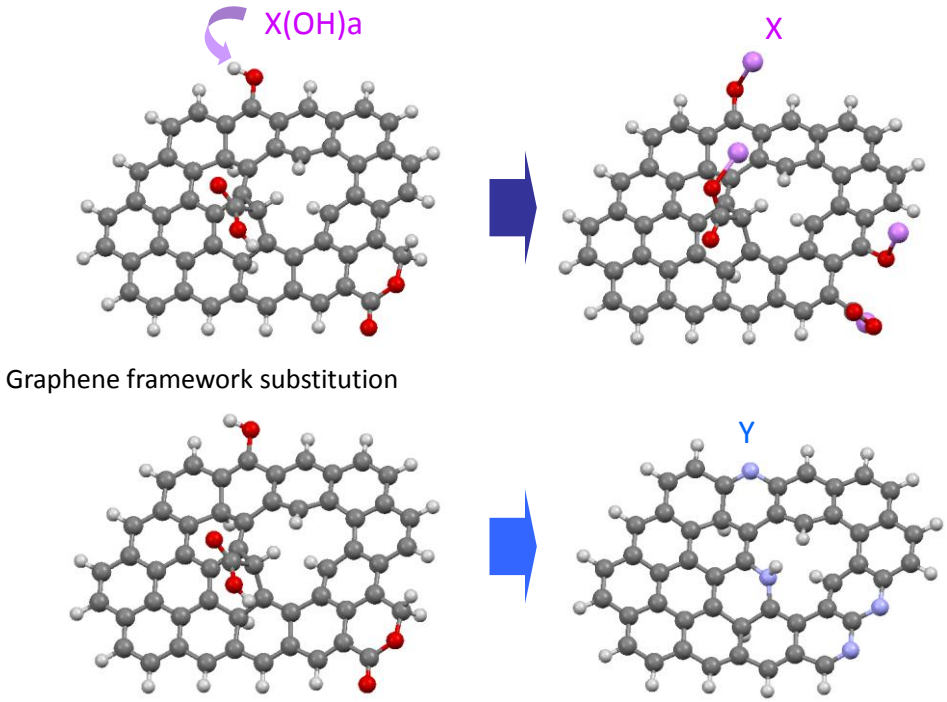

Figure 6.1. Example of types of substitution for carbon material, other metal doping and framework substitution.

List of Publications

Included in this thesis

Synthesis of KOH-activated porous carbon materials and study of hydrogen adsorption
Ai Minoda, Shinji Oshima, Iki Hideshi, Etsuo Akiba
Journal of Alloys and Compounds, **2013**, *580*, S301–S304.

Hydrogen storage capacity of lithium-doped KOH activated carbons
Ai Minoda, Shinji Oshima, Iki Hideshi, Etsuo Akiba
Journal of Alloys and Compounds, **2014**, *606*, 112–116.

Not Included in this thesis

One-Pot, Template Syntheses of a New Class of Metallomacrocycles with a Tetraoxime Cyclic Skelton
S. Tashiro, A. Minoda, M. Yamada, M. Shionoya
Inorg. Chem. **2009**, *48*, 10093-10101.

Synthesis of Vanadium-Doped Palladium Nanoparticles for Hydrogen Storage Materials
Y. Yamamoto, M. Miyachi, Y. Yamanoi, A. Minoda, S. Maekawa, S. Oshima, Y. Kobori, and H. Nishihara
J. Nanopart. Res. **2011**, *13*, 6333-6338.

Metallo-Foldamers with Backbone-Coordinative Oxime-Peptides: Control of Secondary Structures
S. Tashiro, K. Matsuoka, A. Minoda, M. Shionoya
Angew. Chem., Int. Ed. **2012**, *51*, 13123-13127.

Synthesis of Diazenido-ligated Vanadium Nanoparticles
M. Miyachi, Y. Yamamoto, Y. Yamanoi, A. Minoda, S. Oshima, Y. Kobori,, and H. Nishihara
Langmuir, **2013**, *29*, 5099-5103.

Nanoparticle Assemblies via Coordination with a Tetrakis(terpyridine) Linker Bearing a Rigid Tetrahedral Core
Y. Yamanoi,, Y. Yamamoto, M. Miyachi, M. Shimada, A. Minoda, S. Oshima, Y. Kobori, and H. Nishihara
Langmuir, **2013**, *29*, 8768–8772.

Synthesis and Hydrogen Storage Properties of Palladium Nanoparticle-Organic Frameworks
Y. Yamanoi, Y. Yamamoto, M. Miyachi, M. Shimada, A. Minoda, S. Oshima, Y. Kobori, and H. Nishihara
J Inorg Organomet Polym ,**2014**, *24*, 208-213.

Appendix

Nitrogen adsorption measurement analysis

BET method: Brunauer, Emmett and Teller (BET) method used to describe specific surface area:

$$\frac{1}{W\left(\left(P_0/P\right)-1\right)} = \frac{1}{W_m C} + \frac{C-1}{W_m C}\left(\frac{P}{P_0}\right)$$

W= weight of gas adsorbed

P/P_0 = relative pressure

W_m = weight of adsorbate as monolayer

C = BET constant

MP method includes the ability to obtain the micropore volume, surface area, and the pore size distributions from one experimental isotherm. The volume of pores is given by:

$$V = 10^{-4}(S_1 - S_2)\frac{(t_1 + t_2)}{2} \ \text{cm}^3/\text{g}$$

S = total surface area

and the pore size is given by:

$$t = 3.54\frac{W_a}{W_m} \ (\text{Å})$$

DR method allows to calculate the micropore volume from the adsorption isotherm. The total micropore volume can be determined by:

$$\log W = \log\left(\tilde{V}_0 \rho\right) - k\left[\log\left(\frac{P_0}{P}\right)\right]^2$$

W = weight of gas adsorbed

ρ = liquid adsorbate density

$\tilde{V}_0$ = micropore volume

$$k = 2.303K\left(\frac{RT}{\beta}\right)^2$$

P/P_0 = relative pressure

Acknowledgments

The author is sincerely grateful to her supervisor, Professor Etsuo Akiba, for his fruitful advices and encouragements. She deeply thanks Dr. Junko Matsuda of Kyushu University for her valuable insights.

She thanks Dr. Noriko Yoshizawa and Dr. Hideyuki Takagi of the National Institute of Advanced Industrial Science and Technology (AIST) for providing TEM images and TPD measurement data.

She gratefully thanks Professor Hiroshi Nishihara of University of Tokyo for his encouragements. She gratefully thanks Professor Mitsuhiko Shionoya of University of Tokyo for his encouragements and support.

She thanks Dr. Yoshihiro Kobori of JX Nippon Oil & Energy Corporation for his encouragement and discussions. She thanks Dr. Seiji Maeda of JX Nippon Oil & Energy Corporation for his support. She thanks Dr. Hideshi Iki of JX Nippon Oil & Energy Corporation for his various help. She thanks Mr. Shinji Oshima of JX Nippon Oil & Energy Corporation for his continuous encouragements and leading.

She thanks Environmental Technique Service Co. for synthesis of the activated carbons.

She thanks all members of Akiba laboratory at Kyushu University.

She also thanks all members of Hydrogen group, Frontier Research Laboratory, Central Research Laboratory of JX Nippon Oil & Energy Corporation.

Finally, she thanks her parents for everything.